

Submitted to The Astronomical Journal

Spectroscopy of New High Proper Motion Stars in the Northern Sky. I. New Nearby Stars, New High Velocity Stars, and an Enhanced Classification Scheme for M Dwarfs.

Sébastien Lépine^{1,2,3,4}, R. Michael Rich^{2,5} and Michael M. Shara¹

ABSTRACT

We present spectral classification of 105 northern stars with proper motions larger than $0.5'' \text{ yr}^{-1}$, which were recently discovered by us in a survey of high proper motion stars at low galactic latitudes. The final tally is as follows: 54 M dwarfs, 25 sdK and sdM subdwarfs, 14 esdK and esdM extreme subdwarfs, and 12 DA and DC white dwarfs. Among the most interesting cases, we find one star to be the coolest subdwarf ever reported (LSR2036+5059, with spectral type sdM7.5), and a new M9.0 dwarf only about 6pc distant (LSR1835+3259). Spectroscopic distances suggests that 27 of the M dwarfs, and one of the subdwarfs (LSR2036+5059) are within 25pc of the Sun, making them excellent candidates for inclusion in the solar neighborhood census. Estimated sky-projected velocities suggest that most of our subdwarfs and extreme subdwarfs have halo kinematics. We find that several white dwarfs and non metal-poor M dwarfs also have kinematics consistent with the halo, and we briefly discuss their possible origin.

Subject headings: Solar Neighborhood — Stars: low-mass, brown dwarfs — Stars: subdwarfs — Stars: white dwarfs — Stars: kinematics

¹Department of Astrophysics, Division of Physical Sciences, American Museum of Natural History, Central Park West at 79th Street, New York, NY 10024, USA.

²Visiting Astronomer, Lick Observatory.

³Visiting Astronomer, MDM Observatory.

⁴Visiting Astronomer, KPNO.

⁵Department of Physics and Astronomy, University of California at Los Angeles, Los Angeles, CA 90095, USA.

1. Introduction

The current census of stars in the Solar Neighborhood (the volume of space within $\approx 25\text{pc}$ of the sun) is believed to be significantly incomplete, especially at the faint end of the luminosity function. Despite the fact that increasing numbers of substellar objects (L dwarfs, T dwarfs), and low mass stars (M7-M9 dwarfs) are now being discovered with the help of large infrared surveys (Kirkpatrick *et al.* 1999; Delfosse *et al.* 1999; Gizis & Reid 1997) there remain significant numbers of red dwarfs and white dwarfs which are still unaccounted for (Henry *et al.* 1997).

Nearly all the local M dwarfs and white dwarfs are expected to be brighter than magnitude ~ 20 in the optical bands. The majority of them should be detectable as stars with large proper motions. If they haven't been identified yet it is because existing all-sky surveys of high proper motion stars (Luyten 1979, 1980) are themselves significantly incomplete (Scholz *et al.* 2000; Lepine, Shara, & Rich 2002b). Furthermore, the classification and characterization of even the known high proper motion stars is still under way (Gizis & Reid 1997; Jahreiss *et al.* 2001; Reid, Kilkenny, & Cruz 2002).

Recently, several new additions to the solar neighborhood have been confirmed from follow-up observations of newly discovered high proper motion stars (Phan-Bao *et al.* 2001; Henry *et al.* 2002; Scholz *et al.* 2002a; Reylé *et al.* 2002). Follow-up observations of faint stars with large proper motions have also revealed the existence of previously unreported types of objects like a very cool extreme subdwarf (Schweitzer *et al.* 1999), a magnetic DZ white dwarf (Reid, Liebert, & Schmidt 2001), and a pair of nearby cool white dwarfs (Scholz *et al.* 2002b).

In a previous paper (Lepine, Shara, & Rich 2002b) we have reported the discovery of 140 new stars with proper motions larger than $0.5'' \text{ yr}^{-1}$ at low galactic latitudes in the northern sky. For the past two years, we have been carrying a large spectroscopic survey of the new high proper motion stars that we are finding in the northern sky. The spectroscopy is being performed at the Lick Observatory, the MDM Observatory, and the Kitt Peak National Observatory. This first paper of a series presents spectral classification of a first set of 105 stars, all of which are listed in Lepine, Shara, & Rich (2002b). Observations are described in §2. In §3, we describe our classification method, which expands on previous spectral index methods. Calculation of the spectroscopic distances is detailed in §4, where we also discuss the estimated transverse velocities of the stars. Especially interesting or intriguing objects are discussed in §5. Important results are briefly summarized in §6.

2. Spectroscopic observations

Spectra were obtained on six separate runs, at the Lick Observatory in August 2000, July 2001, and December 2001, at the MDM Observatory in February 2001, and May 2002, and at the Kitt Peak National Observatory in May 2002. All 64 Lick spectra were obtained with the KAST spectrograph, mounted at the Cassegrain focus of the 3m Shane Telescope. We imaged the stars through a 2.5" wide slit, onto the 600 l/mm grating blazed at 7500Å. The KAST camera uses a thinned CCD which displays significant fringing redwards of 7500Å, and special care was needed to account for the fringing (using extra dome flats), although some spectra appear to show residuals from the fringing pattern on the far red side. The instrument rotator was used to orient the slit vertically on the sky, to minimize slit loss due to atmospheric diffraction. Standard reduction was performed with IRAF, including sky subtraction, normalization, and removal of telluric lines. The calibration was done using a set of KPNO spectrophotometric standards (Massey *et al.* 1988; Massey & Gronwall 1990). The resulting spectra cover the range 6200-9000Å with a resolution of 2.34Å per pixel.

The first 34 MDM spectra (February 2001) were obtained with the Mark III Spectrograph mounted on the 2.4m Hiltner Telescope. Stars were imaged through a 1.5" slit, onto the 600 l/mm grating blazed at 5800Å. We used a thinned CCD camera (called “Echelle”) which shows only slight fringing in the red. Standard reduction was performed with IRAF, including sky subtraction, normalization, and removal of telluric lines. For calibration, we used the same set of KPNO spectrophotometric standards that we used for the Lick observations (see above). The resulting spectra cover the range 5200-8800Å with a resolution of 2.55Å per pixel. Because of the lower sensitivity of the setup to light redwards of 8000Å, the spectra are very noisy beyond that limit. Because of variable conditions in some of the nights, removal of telluric lines was sometimes difficult, and residual telluric absorption remains in some of the spectra. On the second MDM run (May 2002) we used the MkIII Spectrograph again, but this time with the 300 l/mm grating blazed at 8000Å, which provided a clearer signal in the red. We also used a thick CCD (“Wilbur”) to avoid problems with fringing. The 5 spectra from the second run cover the range 6000-9900Å with a resolution of 3.10Å per pixel.

Finally, we observed the very faint white dwarf LSR2050+7740 during a run on the Mayall 4m Telescope at the Kitt Peak National Observatory. We used the RC Spectrograph with the LB1A camera. Stars were imaged through a 2.0" slit onto the 316 l/mm grating blazed at 7500Å (#BL181). The star was observed near the meridian with the slit oriented north-south to minimize slit loss due to atmospheric diffraction. Standard reduction was performed with IRAF, including sky subtraction, normalization with the KPNO spectrophotometric standards, and removal of telluric lines. The resulting spectrum covers the

range 5800-9100Å with a resolution of 1.74Å per pixel.

3. Spectral Classification

3.1. Spectral Indexes and the Metallicity Scale

A well-defined spectral sequence for M dwarfs in the red part of the spectrum (6000Å-9000Å) was compiled by Kirkpatrick, Henry, & McCarthy (1991). This sequence has become the standard reference for the spectral classification of M dwarfs. Classification on this system is typically performed by fitting the spectrum of a star to this sequence, either by eye or numerically through minimization methods. However, since the work of Reid, Hawley, & Gizis (1995), spectral indexes that measure the depth of various molecular bandheads are being used to provide a quantitative spectral classification of M dwarfs. Spectral indexes have been defined, and their values calibrated against spectral type, by Reid, Hawley, & Gizis (1995) for classification of M dwarfs in the Palomar-MSU spectroscopic survey, by Kirkpatrick, Henry, & Simons (1995) for the classification of late-type M dwarfs, by Kirkpatrick *et al.* (1999) for the classification of late-type M dwarfs and L dwarfs, by Martín *et al.* (1999) also for the classification of late-type M dwarfs and L dwarfs, and by Hawley *et al.* (2002) for the classification of M dwarfs found in the Sloan Digitized Sky Survey. A total of 45 different spectral indexes are defined in the 5 papers quoted above. All of them are correlated with spectral type, though some provide a better diagnosis than others.

A very useful classification scheme was developed by Gizis (1997, hereafter G97), based on four of the Reid, Hawley, & Gizis (1995) spectral indexes (CaH1, CaH2, CaH3, TiO5). Several authors have performed spectral classification using this system (Gizis & Reid 1997; Schweitzer *et al.* 1999; Jahreiss *et al.* 2001; Cruz & Reid 2002). The G97 method separates red dwarfs into three metallicity classes: dwarfs (dM or M), subdwarfs (sdM), and extreme subdwarfs (esdM). It also yields a good spectral classification for sdM, esdM and early/intermediate M dwarfs, but is not appropriate for the classification of late-type M dwarfs because the four indexes measure the strength of molecular features around 7000Å which tend to saturate beyond spectral type M6. Classification of late-type M dwarfs can be performed using the spectral indexes defined in Kirkpatrick *et al.* (1999) and Martín *et al.* (1999), or by using the single index defined by Kirkpatrick, Henry, & Simons (1995). We maintain, however, that an improved and unified scheme for the quantitative classification of all M dwarfs is needed.

Here we expand on the G97 method, and define a set of spectral indexes which measure most major features in the 6000Å-9000Å spectral range (see Table 1). In Figure 1, we

show the spectral features measured by each individual index. From G97, we adopt the CaH1, CaH2, CaH3 indexes (which measure the strength of the CaH bands blueward of 7050Å) and the TiO5 index (which measures the TiO bandhead redward of 7050Å). From Hawley *et al.* (2002), we adopt the VO 7434 and TiO 8440 indexes (renamed VO1 and TiO7, respectively) which measure the strength of the VO band redward of 7530Å and the TiO bandhead blueward of 8430Å. We introduce two new indexes, TiO6 which measures the depth of the prominent TiO bandhead redward of 7600Å, and VO2, which measures the tail of that same TiO bandhead blended with the VO band feature redward of 7850Å which is very prominent in late-type M dwarfs. Our VO2 index is similar to the VO 7912 index defined in Hawley *et al.* (2002), but the reference level (denominator) is defined around 8140Å instead of 8410Å; we prefer to use a reference level that is closer on the spectrum to the measured feature. Finally, we define a new Color-M index which measures the slope of a pseudo-continuum using reference points defined in narrow spectral ranges with a local maximum in intensity. This color index is very useful in estimating the general shape of the spectral energy distribution.

As a first step, we follow the prescription of G97 to separate our red dwarf stars into the three metallicity classes. We assume that all the stars in our list are gravitationally bound to the galaxy, which means they cannot have a transverse velocity larger than 500 km/s. Because our targets all have proper motions larger than 0.5 arcsec/yr, they must be within 200 pc of the sun, which means a distance modulus smaller than 6.5. Since all our stars have an apparent red magnitude larger than 12, this means none of our stars can have an absolute magnitude brighter than 5.5, and most are much fainter. This completely rules out the possibility that any of these stars are giants or supergiants.

The separation into M, sdM, and esdM classes is based on the ratio of the CaH band indexes to the TiO5 index (see Figure 2). We use the relationships defined in G97 for the separation of the stars into the different classes; these relationships are illustrated on Figure 2. To be considered an sdM/esdM, a star has to be within the limits defined by G97 in at least two of the diagrams. The low value of the CaH1 index for three late-type M dwarfs ($\text{TiO5} < 0.35$) results from a low signal-to-noise ratio in those stars around where CaH1 is measured. The CaH2/TiO 5 relationship was used to separate the esdM from the sdM. For the late K dwarfs and early M dwarfs, the G97 molecular bands criteria are more ambiguous; the CaH indexes and the TiO5 index all converge to 1 toward earlier spectral types. There appear to be a number of stars with $\text{TiO5} > 0.7$ that could be M dwarfs. However, these would have a spectral type earlier than M2, which means they would have an absolute magnitude $M_R < 8$. However, if they are M dwarfs they would be too faint ($R > 14$) to be within a few hundred parsecs. Because of their large proper motions ($\mu > 0.5'' \text{ yr}^{-1}$) these M dwarfs would have extremely large transverse velocities ($V_T > 500 \text{ km s}^{-1}$). For these reasons, it is likely

that these stars are relatively nearby subdwarfs, instead of very distant, very high-velocity dwarfs.

3.2. M dwarfs

Our spectral types for the M dwarfs are assigned based on our expanded classification scheme which uses all the indexes defined in Table 2. We have kept the relationships defined by G97 for the CaH2, CaH3, and TiO5 indexes. The spectral type S_P correlates with these indexes as:

$$S_P = 7.91 \text{ CaH2}^2 - 20.63 \text{ CaH2} + 10.71 \quad (\text{M0} - \text{M6}) \quad (1)$$

$$S_P = -18.00 \text{ CaH3} + 15.80 \quad (\text{M0} - \text{M6}) \quad (2)$$

$$S_P = -9.64 \text{ TiO5} + 7.76 \quad (\text{M0} - \text{M6}) \quad (3)$$

We give in parentheses the range over which these relationships are valid. There are weaknesses to these indexes which we now note, as a prelude to an improved classification system given below. First, the three indexes above do not make use of the full spectral range 6000Å-9000Å where several strong molecular bands are found in M dwarfs. Second, the CaH2, CaH3 and TiO5 indexes are defined in a low-intensity region of the optical spectral energy distribution (for intermediate and late-type dwarfs). A third problem is that they are not strictly strictly independent, since CaH2, CaH3, and TiO5 all use the same pseudo-continuum region as their reference point (7042Å-7046Å). This reference region is only 4Å wide, and is therefore sensitive to spectral noise; any significant instrumental deviation in the 7042Å-7046Å region propagates equally in all three indexes.

To derive the correlations for the other indexes, we first obtained a crude spectral typing by visual inspection of the spectra and comparison with the Kirkpatrick, Henry, & McCarthy (1991) sequence. We then made fine corrections to the spectral types (typically by no more than one subtype), until we obtained a clean sequence where all indexes were linearly correlated with spectral type. The final sequence is shown in Figure 3. The few outlying points in the graphs are associated with stars for which we only have a noisy spectrum (especially LSR0212+7012, LSR0200+5530, and LSR0646+3412). We used linear regressions to obtain the following relationships:

$$S_P = -30.5 \text{ VO1} + 32.2 \quad (\text{M2} - \text{M8}) \quad (4)$$

$$S_P = -11.2 \text{ TiO6} + 11.9 \quad (\text{M2} - \text{M8}) \quad (5)$$

$$S_P = -10.5 \text{ VO2} + 12.4 \quad (\text{M3} - \text{M9}) \quad (6)$$

$$S_P = -11.0 \text{ TiO7} + 13.7 \quad (\text{M3} - \text{M9}) \quad (7)$$

Again we give in parentheses the range over which each of the relationship is valid. The VO1, TiO6, VO2, and TiO7 relationships are valid for later spectral types than the CaH2, CaH3, and TiO5 relationships. The indexes, taken together, can be used to obtain spectral types over the whole M dwarf range to an accuracy of about half a spectral type.

While the variation of all the spectral indexes with spectral type appears to be linear, there appears to be an exponential progression of the Color-M index over the M dwarf sequence. In Figure 3, we plot the logarithm of the Color-M index, and show that it can be fitted with a linear relationship in the M3-M8 range. The Color-M uses two spectral regions separated by more than 1500Å and is thus not as reliable as the other indexes for spectral classification purposes, as it is more sensitive to slit loss, extinction, and other calibration errors. Nevertheless, the correlation is reasonably good, and the Color-M index may be used to help determine the spectral type of intermediate M dwarfs (M4-M8) using the relation:

$$Sp = 7.5 \log(\text{Color} - M) + 1.6 \quad (\text{M4} - \text{M8}) \quad (8)$$

The complete sequence of M dwarf spectra is displayed in Figures 4-5. One can verify that there is a smooth, continuous evolution toward later types.

We further examined the spectra for any indication of H_α ($\lambda 6563$) in emission. Given the quality and resolution of the spectra, we determined that H_α detection could be considered significant if it had an equivalent width smaller than about -2.0Å. We added the subscript e to stars which qualified as H_α emitters under this criterion. Close observation of the spectra suggests that several more stars (including all those of spectral type 6.0 and later) may also be H_α emitters, but the equivalent width of the H_α line was too weak to be considered significant under the criterion above. High resolution observations of the spectral region around 6565Å would be required in order to determine which stars can be considered to be emission-line stars in a broader sense. It is remarkable that we find only 8 emission-line stars in our sample of 54 M dwarfs, especially given the large number of M5-M6 stars in the sample. Generally, about half of the M5-M6 dwarfs are found to be active (see Gizis *et al.* (2000) 2000, and references therein). Because activity is correlated with age, this is an indication that the stars in our sample tend to be relatively old for M dwarfs. This is consistent with the relatively larger velocities that we find for most of them (see §4.3 below).

3.3. Subdwarfs and extreme subdwarfs

For sdM stars, we simply follow the G97 classification system, which uses only the CaH2 and CaH3 indexes:

$$S_P = 7.91 \text{ CaH2}^2 - 20.63 \text{ CaH2} + 10.71 \quad (9)$$

$$S_P = -16.02 \text{ CaH3} + 13.78 \quad (10)$$

We plot the distribution of CaH1, CaH2, and CaH3 values as a function of the sdM subtype in Figure 6. Because the TiO and VO bands are very weak in subdwarfs, they cannot be used as classification criteria. The Color-M term again appears to increase exponentially with the subtype, loosely following the relationship:

$$Sp = 7.3 \log(\text{Color} - M) - 0.6 \quad (11)$$

As expected, the slope of the pseudo-continuum measured by Color-M is significantly shallower for a given subtype than it is for the M dwarfs. The complete sequence of sdM spectra is displayed in Figure 7. One of our subdwarfs is classified with a very late spectral type sdM7.5. To the best of our knowledge, this is the coolest subdwarf ever identified.

For esdM stars, we also use the G97 calibration based on the CaH2 and CaH3 indexes.

$$S_P = 7.91 \text{ CaH2}^2 - 20.63 \text{ CaH2} + 10.71 \quad (12)$$

$$S_P = -13.47 \text{ CaH3} + 11.50 \quad (13)$$

We plot the distribution of CaH1, CaH2, and CaH3 values as a function of the sdM subtype in Figure 8. The Color-M term is again correlated with spectral type, following approximately the relationship:

$$Sp = 22.0 \log(\text{Color} - M) - 4.1 \quad (14)$$

Many of our esdM spectra (especially those from the 2001 MDM run) are relatively noisy in the red beyond 8000Å. For this reason, the Color-M index is not very reliable for those stars. The 3 points in the bottom panel of Figure 8 that lie well outside the relation defined in equation 14 are from noisy MDM spectra. We suspect that the correlation between the esdM subtype and the Color-M index is actually very well defined. Spectra obtained with minimal slit loss and which are carefully normalized are, of course, required if the Color-M index is to be used for the classification of esdM stars. The complete sequence of esdM spectra is displayed in Figure 9.

3.4. White Dwarfs

The white dwarf stars in our sample are easily identified because they show none of the molecular features observed in the dwarf stars. We compared our spectra to the catalog compiled by Wesemael (1993). We examined the spectra to determine if H_{α} , or any other line, was present in absorption. The 12 white dwarfs in our sample are either completely featureless (DC stars) or display some weak H_{α} emission (DA stars).

Following the observational fact that the spectral subtype of a white dwarf goes as $50,400/T_{eff}$, we made blackbody fits of our white dwarf spectra in the 6000Å-9000Å range. The corresponding blackbody temperatures are given in Table 3. The fits are accurate to ± 250 K, and the spectral typing is accurate to one spectral subtype. All the stars in our sample are late-type DA or DC white dwarfs, with DC7 being the earliest, and DC10 the latest. Our spectra for the white dwarf stars are plotted in Figure 10. Because we used observational setups optimized for the observation of red dwarf stars, our white dwarf spectra are sometimes very noisy, and the classification is not very reliable. The assignment of white dwarfs in the DC class is particularly dubious, and may simply result from our inability to detect the H_{α} absorption line in noisy spectra. Still, our spectra clearly show that all the white dwarfs discovered in the sample are relatively cool, old objects.

4. Kinematics and Distances

4.1. Reduced proper motion diagrams

A most useful tool for pre-selecting classes of high proper motion stars is the reduced proper motion diagram. Recently, Salim & Gould (2002) have demonstrated that dwarfs, subdwarfs, and white dwarfs can be separated out when the ratio of infra-red to optical colors is used in making the reduced proper motion diagrams. The reduced proper motion H is obtained by adding the logarithm of the proper motion to the apparent magnitude of the star (Luyten 1925). Here we use two different reduced proper motion terms:

$$H_R \equiv R + 5 + 5 \log \mu = M_R + 5 \log v_t - 3.38 \quad (15)$$

$$H_{K_s} \equiv K_s + 5 + 5 \log \mu = M_{K_s} + 5 \log v_t - 3.38 \quad (16)$$

Because both the apparent magnitude (R, K_s) and proper motion (μ) are a function of the distance to the star, the distance terms cancel, and so the reduced proper motion really is a measure of the combined absolute magnitude (M_R, M_{K_s}) and transverse velocity (v_t). Reduced proper motion diagrams are plots of the reduced proper motion against a color term.

We have made reduced proper motion diagrams using $[M_R, B-R]$ and $[M_{K_s}, R-K_s]$. In Figure 11, we plot the stars for which the corresponding magnitudes are available, using different symbols for the different classes of objects: filled circles for M dwarfs, open squares for sdM, filled triangles for esdM, and asterisks for the white dwarfs. On the $[M_R, B-R]$ diagram, white dwarfs populate a distinct locus, but it is not possible to distinguish the dwarfs from the subdwarfs. On the $[M_{K_s}, R-K_s]$ diagram however, the dwarfs, subdwarfs, and white dwarfs clearly occupy different loci. Proper motion and optical+infrared photometry alone can thus be used to guess what class of object one is dealing with, although spectroscopic confirmation is still required for certainty. This however, is a very useful method for pre-selecting stellar populations for follow-up observations.

4.2. Spectroscopic distance estimates

To obtain a calibration of the absolute magnitude against spectral type for M dwarfs, we used a set of nearby stars for which there exist parallax measurements accurate to better than 10%. We selected 55 stars from the NSTARS database (<http://nstars.arc.nasa.gov>) spanning a range of spectral types from M0.5 V to M8.0 V. There were very few objects in the M7.0 to M9.0 range, so we complemented the sample with 12 late-type dwarfs ranging from M6.5 V to M9.5 V whose parallaxes are given in Dahn *et al.* (2002). We proceeded to recover the B, R, and K_s magnitudes of those stars *using the same sources as those used for our sample of new high proper motion stars*, namely the Guide Star Catalog-II (GSC2.2.1) for the B and R magnitudes, and the 2MASS Second Incremental Release for the K_s magnitude. This procedure guarantees that the stars can then be compared on exactly the same magnitude system. While not all the stars had counterparts in the GSC2.2.1 or 2MASS, we did obtain reference magnitudes for at least 35 stars in each band. We then used the parallax measurements to derive a spectral-type / absolute magnitude calibration.

The correlations between spectral type and absolute magnitudes are shown in Figure 12. The relationship is clearly not linear across the M dwarf sequence, as the absolute B and R magnitudes drop quickly between spectral types M4 and M6; the absolute K magnitude also appears to drop faster between M3 and M5. We found that the overall behavior of the correlations could be modeled using third order polynomials. We performed χ^2 minimization fit to obtain the following empirical relationships between spectral types (S_P) and absolute magnitudes:

$$S_P(M) = 0.0156 M_B^3 - 0.730 M_B^2 + 11.8 M_B - 60.4 \quad (17)$$

$$S_P(M) = 0.0143 M_R^3 - 0.531 M_R^2 + 7.02 M_R - 28.1 \quad (18)$$

$$S_P(M) = 0.0974 M_{K_s}^3 - 2.076 M_{K_s}^2 + 15.4 M_{K_s} - 35.9. \quad (19)$$

We then used equations 17-19 to derive reference absolute magnitudes for each given spectral type S_P , and used these to obtain a spectroscopic distance estimate for each of our M dwarfs. Results are listed in Table 1. For stars with magnitudes in more than one band, the average distance is used; distance estimates in the different bands usually agreed to better than 30%.

We use the same method to determine a spectral-type / absolute magnitude calibration for sdM and esdM stars. We used as reference a set of 25 sdM and 19 esdM stars with spectral type and geometric parallax given in G97. We looked for counterparts of these stars in the Guide Star Catalog-II (GSC2.2.1), and the 2MASS Second Incremental Release. The empirical spectral-type / absolute magnitude relationships are plotted in Figures 13-14. In all cases, the relationships appear to be linear. We thus performed χ^2 minimization fit of first order polynomials to obtain the following empirical relationships between spectral types (S_P) and absolute magnitudes. For the subdwarfs (sdM), we find:

$$S_P(\text{sdM}) = 1.12 M_B - 12.4 \quad (20)$$

$$S_P(\text{sdM}) = 1.13 M_R - 10.0 \quad (21)$$

$$S_P(\text{sdM}) = 1.65 M_{K_s} - 10.4. \quad (22)$$

And for the extreme subdwarfs (esdM), we find:

$$S_P(\text{esdM}) = 1.85 M_B - 23.2 \quad (23)$$

$$S_P(\text{esdM}) = 2.05 M_R - 21.4 \quad (24)$$

$$S_P(\text{esdM}) = 2.68 M_{K_s} - 21.6. \quad (25)$$

Distances for the sdM and esdM stars in our sample are based on the empirical relationships. Estimated values are given in Table 1.

We noted that the spectroscopic distances of several early-type M stars in our list are close to or above 200pc. Because all the stars in our sample have proper motions larger than $0.5'' \text{ yr}^{-1}$, any star at a distance $d > 200\text{pc}$ must be moving relative to the sun with a transverse (sky projected) velocity $V_T = 4.7 \times d \times \mu > 470 \text{ km s}^{-1}$. A star with such a large transverse velocity is very likely to be moving at larger than the Galactic escape speed. It is thus very possible that those distances are overestimated (see subsection below). The most obvious reason for an overestimate in the spectroscopic distance of an early-type star is an incorrect assignment of the spectral class. A comparison of Figures 12-14 shows that early-type esdM stars are systematically fainter (up to 2 magnitudes) than sdM stars, and sdM stars are themselves systematically fainter (also by up to 2 magnitudes) than M dwarfs. It is thus possible that those too-distant M dwarfs are actually closer sdM stars, and that the too-distant sdM are closer esdM. In Table I, we indicate with parentheses the possible change

in spectral class based on the kinematics, and we tabulate two values for the distances, with the shorter estimate corresponding to the lower metallicity class. In all cases, the shorter estimate is consistent with a star that is gravitationally bound to the galaxy (but still with a relatively large transverse velocity).

For the white dwarfs, we obtain crude photometric distances with the B-R color, by using the relation given in Oppenheimer *et al.* (2001):

$$M_B = 12.73 + 2.58(B - R). \quad (26)$$

For those stars for which we do not have B magnitudes, we compare them with other white dwarfs in our sample with similar spectral types and estimate their relative distances based on their relative R magnitudes. Photometric distances for the white dwarfs are listed in Table 1.

4.3. Kinematics

We derive transverse (sky-projected) velocities for all the stars based on their proper motions and spectroscopic distance estimates. The derived values are tabulated in Table 1. We use the assumption that the radial velocity of all the stars is zero, and we determine their corresponding distribution in the UVW velocity space, where U is the velocity toward the galactic center, V is the velocity toward the direction of galactic rotation, and W is the velocity toward the north galactic pole. We plot the distribution in the VW and UW planes in Figures 15 and 16. Because our stars are all located within 25 degrees of the galactic plane, the estimated W velocity component is relatively accurate in the assumption of zero radial velocity. The U and V components, while very approximative, are nevertheless very indicative of the general kinematics for a group of objects.

The transverse velocities that we find for most of our M dwarfs are significantly larger than those expected of young disk stars. This is clearly the result of the proper motion bias of our survey, which tends to select stars with unusually large transverse velocities. This is also consistent with the low numbers of active, emission-line stars that we find in our sample. The distribution of M dwarfs in the VW and UW planes (Figure 15, top) shows that as a group they are consistent with old disk stars. However, we find a significant number of M dwarfs that fall well outside the velocity space limit for disk stars. While they may be extremely rare, the fact that *there exist non metal-poor stars with halo kinematics* requires an interpretation for their origin. Since it is very unlikely that these stars were actually born in the halo, there must be a mechanism that is responsible for sending disk stars into halo-like orbits. Dynamical ejection during promiscuous encounters of binary and single stars in star

clusters is one possibility (Hurley & Shara 2002). Alternatively, these stars could have been accreted from a satellite galaxy in a merger event with the Milky Way. Our current sample of M dwarfs with halo-like kinematics is however relatively small at this point. Clearly, follow-up observations of more faint high proper motion stars are required to discover more of the non-metal poor, high velocity stars, and better characterize their group kinematics.

The velocity space distribution of our 12 white dwarfs is plotted in Figure 15 (bottom panel). Though we have very few objects, it does appear that the white dwarfs have a velocity space distribution that is similar to that of our M dwarfs, with most of them falling within or just outside the limits of disk stars, and a few outliers with halo-like kinematics. While it is tempting to argue that the white dwarfs with the largest space velocities are actually members of the population of old halo white dwarfs claimed by Oppenheimer *et al.* (2001), it is not possible at this point to exclude the possibility that the high velocity white dwarfs are drawn from the same population as those high velocity, non metal-poor M dwarfs. If so, these white dwarfs would not have been born in the halo, but would have gotten there by some dynamical mechanism.

The velocity space distribution of our subdwarfs and extreme subdwarfs (Figure 16, top), on the other hand, is much more consistent with a uniform distribution in the halo, and support the idea that those stars were actually born there. We see no convincing difference between the velocity space distribution of the sdM and esdM stars. Our sample is relatively small however, and a more extensive study of the velocity distribution of a larger sample of low-mass subdwarfs and extreme subdwarfs (complete with radial velocities) would be far more instructive.

We have already mentioned in §4.2 that the spectroscopic distance for some early-type M stars appears to be too large, yielding a velocity that is not consistent with the star being bound to the Galaxy. This problem occurs for 10 sdM subdwarfs, and 2 M dwarfs in our sample. We raise the possibility that these stars have not been assigned to the proper spectral class by the spectroscopic method. The problem with the assignment of spectral class for early-type M dwarfs was already conspicuous in Figure 2. The convergence of the CaH and TiO indexes to a value of 1.0 for warm red-dwarfs makes the separation in the M, sdM, and esdM classes problematic when 6000Å-9000Å spectra are used. The uncertainty with regards to the adopted spectral class leads us to classify these stars as (sd)M or (e)sdM, to emphasize the possibility that the stars may be more metal poor than suggested by the G97 spectral indexes. In Table 1, we list two possible distances (and corresponding sky-projected velocities) for those stars. The larger distance scale (and velocity) corresponds to the spectroscopic distance based on our initial assessment of the spectral class. The shorter distance scale (and velocity) is based on the assumption that the star is more metal poor

than suggested by the spectral indexes (esdM instead of sdM, and sdM instead of M). We plot the UVW velocity-space distribution for those stars in the bottom panel of Figure 15, with the two different distances scales plotted with different symbols. All the stars fall within the limits of the halo kinematics when the short distance scale is used.

If the problem resides with the assignment of the spectral class (which uses the G97 indexes), then the proper motion appears to be the solution in obtaining a better evaluation of the spectral class, provided we use the assumption that all stars must be gravitationally bound to the Galaxy. In this case, these objects are simply metal poor stars with extreme halo kinematics. On the other hand, if we believe that the spectral class assessment with the G97 indexes is accurate, then we have here evidence for a population of stars which are not gravitationally bound to the Galaxy. These could be either transiting extragalactic stars, or Galactic runaways. The fact that most of these high-velocity stars are metal-poor objects would be in better agreement with an extragalactic origin.

5. Notes on Interesting Objects

5.1. LSR0200+5530

With a magnitude $R=19.7$, LSR0200+5530 is the faintest star in our sample. While our MDM spectrum for that star is particularly noisy, it strongly suggests a spectral type M5.5 V. This then places the star at a distance $d=90\text{pc}$, with a surprisingly large transverse velocity $V_T=215\text{ km s}^{-1}$. Thus, LSR0200+5530 appears to be a solar metallicity star with halo kinematics. Since it is unlikely that a non-metal poor star would originate in the halo, this star is most likely to have been born in the disk, and to have migrated to the halo afterward. A close gravitational interaction with a disk binary in a star cluster star may have sent this one flying away. Alternatively, the star could have been accreted by the Galaxy through a merger event, and be a relic of a former Galactic satellite.

5.2. LSR0310+6634

This cool white dwarf (spectral type DC10) apparently has a very large transverse velocity $V_T=230\text{ km s}^{-1}$ consistent with the kinematics of a halo star. While this star might be a member of the hypothetical population of very old halo white dwarfs suggested by Oppenheimer *et al.* (2001), the fact that we are finding non-metal poor M dwarfs with halo kinematics (e.g. LSR0200+5530 above) suggest that this white dwarf might also have been born in the disk but later migrated to the halo.

5.3. LSR0400+5417

It is unclear whether LSR0400+5417 is a subdwarf (sdK) or an extreme subdwarf (esdK) star. While its spectrum is consistent with an sdK7 subtype, the inferred spectroscopic distance is very large ($d=375\text{pc}$) which yields an incredibly large transverse velocity $V_T=1330\text{ km s}^{-1}$. If this is true, then this metal poor star is an extragalactic object that just happens to be moving through the Galaxy at this time. On the other hand this may actually be an intrinsically fainter esdK7 star at a much closer distance. Based on the extreme subdwarf distance calibration, we estimate that as an esdK7 this star would be at ($d=150\text{pc}$). This reduces the transverse velocity to $V_T=530\text{ km s}^{-1}$, which is still extremely large, but which is almost consistent with the star being in the halo.

5.4. LSR0419+4233

With a spectral type M8.5 Ve, this low-mass star is at a spectroscopic distance of only 10pc. This star has a very large proper motion ($\mu = 1.535''\text{ yr}^{-1}$) which suggest a transverse velocity $V_T = 72\text{ km s}^{-1}$. This is relatively large for a disk star, and one has to wonder if the star may not actually be much closer. This is clearly a high priority target for follow-up parallax measurements.

5.5. LSR0549+2329

This DC8 white dwarf also has a velocity $V_T=260\text{ km s}^{-1}$ that is typical of a star with halo kinematics. Like LSR0310+6634 (see above) it can be considered a halo white dwarf. However, we emphasize again that our discoveries of non metal-poor M dwarfs with similar kinematics (e.g. LSR1722+1004 below) suggests that this may not be a very old object born in the halo, and that its situation in the halo could be relatively recent.

5.6. LSR0556+1144

This relatively bright $R=14.2$ star is the second brightest of the list. With a spectral type M5.5 V, it is also relatively cool and intrinsically faint, and has a spectroscopic distance of only 10pc. This is a good candidate for inclusion in the census of very nearby stars.

5.7. LSR1722+1004

This is another M dwarf with disk-like abundances and halo-like kinematics. Its spectrum is clearly that of a metal-rich M4.0 V, but its spectroscopic distance of $d=70\text{pc}$ implies a transverse velocity $V_T=240\text{km s}^{-1}$. Again, this could be a star initially born in the disk and later ejected out in the halo.

5.8. LSR1802+0028

This extreme subdwarf is very distant (spectroscopic distance $d=180\text{pc}$), and it has an extremely large transverse velocity ($V_T=460\text{km s}^{-1}$). No doubt this is a halo star. Its spectrum actually show very little trace of molecular TiO absorption. This could be an extremely metal poor object.

5.9. LSR1833+2219

This star is a companion to the nearby star GJ718A, also known as the flare star V774 Her. In a previous paper (Lepine, Shara, & Rich 2002a), we named this star GJ718B, and reported a spectral type M4.5 V. This spectral type was based on the G97 indexes alone. The use of our expanded system yields a spectral type M5.0 V instead. The spectroscopic distance of 26pc is very close to the actual distance of 23.4pc measured by HIPPARCOS for GJ718A (Perryman 1997). This supports the idea that our spectroscopic distances are reasonably accurate, at least for the M dwarfs.

5.10. LSR1835+3259

With a spectral type M9.0 V, this star is the coolest one in our sample. Its optical and infrared magnitudes all are consistent with the star being at about 6pc. Only two other M9.0 dwarfs are known to be within 7pc of the sun: DENIS 1048-39 at a distance of about 4pc, and LP944-20 at a distance of about 5pc (Delfosse *et al.* 2001).

5.11. LSR1914+2825AB

This pair of early type subdwarf (sdM) stars is very peculiar because of its large spectroscopic distance. Assuming a distance of 200pc, the pair have a huge transverse velocity of (500km s^{-1}), making them very obvious halo stars. Their angular separation of $\approx 12''$ implies an orbital distance $> 2400\text{AU}$. At a distance of 160pc-200pc (based on the sdM distance scale) they seem to be moving at a velocity close to or larger than the Galactic escape speed. This is why we are suggesting that these stars might be more metal poor and therefore intrinsically fainter than average sdM stars of the same subtype; we classify them as (e)sdM stars. If we use the extreme subdwarfs (esdM) distance scale, we get a distance of about 90pc. This in turn yields a transverse velocity of $250\text{-}275\text{km s}^{-1}$, which is consistent with their being halo stars.

We note that there is a $\sim 25\%$ discrepancy in the estimated spectroscopic distances of the stars if we calibrate them on the sdM scale (200pc to 160pc). We do not have 2MASS K_s magnitudes for those stars, and we must rely on the B and R photographic magnitudes estimated from the POSS-II plates. Because the photographic magnitudes are accurate to about 0.5 mags, we can expect a 25% error in the relative distance estimate of the stars, which is actually what we have. However, it is interesting to note that the discrepancy in the spectroscopic distances shrinks to only 10% (110pc to 100pc) when we calibrate them on the esdM distance scale. This better agreement independently suggest that the two stars indeed may be extreme subdwarfs.

5.12. LSR1928-0200AB

The spectroscopic distances estimated for the stars in this pair show a 30% discrepancy. The earlier M3.5 V component LSR1928-0200A has a spectroscopic distance of 85pc, and the later M5.5 V component LSR1928-0200B has spectroscopic distance of 65pc. These relatively large distances translate into extremely large transverse velocities ($V_T=260\text{-}340\text{ km s}^{-1}$) for non metal-poor stars.

It is possible to resolve both the discrepancy in the relative distances of the components by assuming that the stars are somewhat metal poor, though perhaps not enough to be classified as sdM stars. If LSR1928-0200A was an sdM3.5 subdwarf, its spectroscopic distance would be significantly shorter (40pc). As an sdM5.5, LSR1928-0200B would be a little shorter (55pc). Clearly, by having the two stars in an intermediate state between dwarf and subdwarf, it would be possible to obtain an agreement in their distances, which would be around 60pc. The system would then still have a very large transverse velocity ($V_T=240\text{ km}$

s^{-1}) more typical of a halo star.

How can a slightly metal poor binary system have halo kinematics? The fact that this is long period binary seems to be at odd with the hypothesis that it got ejected from the disk through a close gravitational encounter, though a complex multi-body dynamical event in a cluster cannot be ruled out. The system could also be on a highly eccentric galactic orbit from a dynamically violent birth. A more conservative scenario is that this system has been accreted by the Galaxy, possibly through a merger event with a slightly metal poor galaxy or cluster.

5.13. LSR1945+4650AB

This is a pair of cool white dwarfs (DA9+DC10) for which we are having some problem in estimating their distance. The photometric distance derived for LSR1945+4650A (30pc) is half the photometric distance of its companion (60pc). The two stars are a common proper motion pair, and the chances are extremely small that they are not physically related. The discrepancy in the estimated photometric distances rather suggests that the method is prone to errors. The photometric distance is based on the B-R color term (Equation 26). Both B and R are derived from photographic plates, and accurate to only about 0.5 magnitudes. Therefore, B-R is accurate to about 0.7 magnitudes, which can lead to a 40% error in the distance estimate of a single object, which means that there typically is a factor 2 error in the relative estimated distance between two stars.

5.14. LSR2036+5059

We find for this star a spectral type sdM7.5, which is unusually late for a subdwarf. As far as we know, LSR2036+5059 is the coolest M subdwarf reported to date. The coolest subdwarf reported in the literature so far was LHS377, with a spectral type sdM7.0 (Gizis 1997). The spectrum of this star is distinctly odd-looking with its very deep CaH band and relatively weak TiO features (see Figure 7). With a transverse velocity of $\sim 90 \text{ km s}^{-1}$, it is a possible member of the old-disk population. This star could have a mass extremely close to the hydrogen burning limit for metal poor stars. At a spectroscopic distance of only 18pc, this subdwarf is also a very likely member of the Solar Neighborhood.

5.15. LSR2122+3656

This star, with spectral type esdM5.0, is the coolest extreme subdwarf in our sample. It is also the closest, at a spectroscopic distance of 45pc. This emphasizes the extreme rarity of the esdM stars in the Solar Neighborhood, and shows the effectiveness of high proper motion surveys in recovering them.

5.16. LSR2124+4003

This cool red dwarf (M6.5 V) was among the brightest stars in our sample ($R=14.9$). With a spectroscopic distance of about 7pc, it may prove to be among the 100 nearest systems. Along with LSR1835+3259, this is a top candidate for follow-up, astrometric parallax measurements.

6. Conclusions

We have obtained spectra for 105 new stars with large proper motions ($\mu > 0.5'' \text{ yr}^{-1}$) found at low galactic latitudes (Lepine, Shara, & Rich 2002b). We find that 54 of the targets are M dwarfs (M), 25 are subdwarfs (sdK, sdM), 14 are extreme subdwarfs (esdK, esdM), and 12 are late-type DA and DC white dwarfs.

We have expanded the G97 classification method for M dwarfs and subdwarfs by defining a larger set of spectral indexes whose calibration with spectral type can be used for spectral classification. The new scheme can be applied to perform spectral classification of all M dwarfs (early and late-type), subdwarfs, and extreme subdwarfs, from a spectrum of the 6000Å-9000Å wavelength range. Among the M dwarfs classified in this paper, 8 have a spectral subtype M7 and later, including one new M9.0 star. We also find one subdwarf with a very late spectral type of sdM7.5, the coolest subdwarf ever reported.

We have provided a crude classification of the 12 white dwarf stars, from blackbody fits of the spectral energy distribution in the 6000Å-9000Å range. All the white dwarfs are relatively cool DA and DC, with the warmest at DC8 (6500K) and the coolest at DC11 (4750K). Many of the DC spectra are relatively noisy, and the DC spectral class was assigned only by default, for lack of clear identification of H_α absorption. We thus suspect some of our DCs are likely to be unrecognized DAs.

We have derived a spectral-type / absolute magnitude calibration using sets of M, sdM, and esdM stars with published geometric parallaxes. We have found the counterparts of

those stars in the Guide Star Catalog-II (GSC2.2.1) and in the 2MASS Second incremental Release, to obtain their observed B, R, and K_s magnitudes. The spectral-type / absolute magnitude relationships for M dwarfs was modeled with a third order polynomial, while we fit a linear relationship for the sdM and esdM stars. Using the empirically determined spectral-type / absolute magnitude relationships, we have determined spectroscopic distances for all the observed red dwarfs and subdwarfs.

We have shown that the spectroscopic distances of several early-type stars appear to be overestimated, as they yield sky-projected velocities that far exceed the escape velocity of the Galaxy. This can be explained if the spectral class assignment method, which uses the relative strength of the CaH and TiO bands, fails to properly separate out the M, sdM and esdM stars of early-type. Seemingly unbound stars can be reassigned to a closer distance, and with a reasonably low velocity if we assume that they are more metal poor than suggested by the CaH and TiO indexes.

Follow-up spectroscopy of newly discovered faint stars with large proper motions proves yet again to be very productive in recovering intrinsically faint stars in the Solar neighborhood, and faint stars with extreme transverse velocity components (possibly halo stars). Our spectroscopic follow-up survey of new high proper motion stars is still in progress, and is being expanded as new northern stars with large proper motions are being discovered. Future results will be presented in upcoming papers in this series.

This research program is being supported by NSF grant AST-0087313 at the American Museum of Natural History, as part of the NSTARS program.

This work has been made possible through the use of the Guide Star Catalogue-II. The Guide Star Catalogue-II is a joint project of the Space Telescope Science Institute and the Osservatorio Astronomico di Torino. Space Telescope Science Institute is operated by the Association of Universities for Research in Astronomy, for the National Aeronautics and Space Administration under contract NAS5-26555. The participation of the Osservatorio Astronomico di Torino is supported by the Italian Council for Research in Astronomy. Additional support is provided by European Southern Observatory, Space Telescope European Coordinating Facility, the International GEMINI project and the European Space Agency Astrophysics Division.

This publication makes use of data products from the Two Micron All Sky Survey, which is a joint project of the University of Massachusetts and the Infrared Processing and Analysis Center, funded by the National Aeronautics and Space Administration and the National Science Foundation.

The data mining required for this work has been made possible with the use of the SIMBAD astronomical database and VIZIER astronomical catalogs service, both maintained and operated by the Centre de Données Astronomiques de Strasbourg (<http://cdsweb.u-strasbg.fr/>).

REFERENCES

Cruz, K. L., & Reid, I. N. 2002, AJ, 123, 2828

Dahn, C. C., Harris, H. C., Vrba, F. J., Guetter, H. H., Canzian, B., Henden, A. A., Levine, S. E., Luginbuhl, C. B., Monet, A. K. B., Monet, D. G., Pier, J. R., Stone, R. C., Walker, R. L., Burgasser, Adam J., Gizis, J. E., Kirkpatrick, J. D., Liebert, J., & Reid, I. N. 2002, AJ, 124, 1170

Delfosse, X., Tinney, C. G., Forveille, T., Epchtein, N., Borsenberger, J., Fouqué, P., Kimeswenger, S., & Tiphène, D. 1999, A&AS, 135, 41

Delfosse, X., Forveille, T., Martín, E. L., Guibert, J., Borsenberger, J., Crifo, F., Alard, C., Epchtein, N., Fouqué, P., Simon, G., & Tajahmady, F. 2001, A&A, 366, L13

Gizis, J. E. 1997, AJ, 113, 806 (G97)

Gizis, J. E., & Reid, I. N. 1997, PASP, 109, 849

Gizis, J. E., Monet, D. G., Reid, I. N., Kirkpatrick, J. D., Liebert, J., & Williams, R. J. 2000, AJ, 120, 1085

Henry, T. J., Ianna, P. A., Kirkpatrick, J. D., & Jahreiss, H. 1997, AJ, 114, 388

Henry, T. J., Walkowicz, L. M., Barto, T. C., & Golimowski, D. A. 2002, AJ, 123, 2002

Hawley, S. L., *et al.* 2002, AJ, 123, 3409

Hurley, J. R., Shara, & M. M. 2002, ApJ, 570, 184

Jahreiss, H., Scholz, R., Meusinger, H., & Lehmann, I. 2001, A&A, 370, 967

Kirkpatrick, J. D., Henry, T. J., & McCarthy, D. W. 1991, ApJS, 77, 417

Kirkpatrick, J. D., Henry, T. J., Simons, D. A. 1995, AJ, 109, 797

Kirkpatrick, J. D., Reid, I. N., Liebert, J., Cutri, R. M., Nelson, B., Beichman, C. A., Dahn, C. C., Monet, D. G., Gizis, J. E., & Skrutskie, M. F. 1999, ApJ, 519, 802

Lépine, S., Shara, M. M., & Rich, R. M. 2002a, AJ, 123, 3434

Lépine, S., Shara, M. M., & Rich, R. M. 2002b, AJ, 124, 1190

Luyten W. J. 1925, ApJ, 62, 8

Luyten W. J. 1979, LHS Catalogue: a catalogue of stars with proper motions exceeding 0.5" annually, University of Minnesota, Minneapolis (*CDS-Vizier catalog number I/87B*)

Luyten W. J. 1980, New Luyten Catalogue of stars with proper motions larger than two tenths of an arcsecond (NLTT), University of Minnesota, Minneapolis (*CDS-Vizier catalog number I/98A*)

Martín, E. L., Delfosse, X., Basri, G., Goldman, B., Forveille, T., Zapatero Osorio, M. R. 1999, AJ, 118, 2466

Massey, P., Strobel, K., Barnes, J. V., Anderson, E. 1988, ApJ, 328, 315

Massey, P., & Gronwall, C. 1990, ApJ, 358, 344

Oppenheimer, B. R., Hambly, N. C., Digby, A. P., Hodgkin, S. T., & Saumon, D. 2001, Science, Volume 292, Issue 5517, pp. 698-702

Perryman, M. A. C. 1997, The Hipparcos and Tycho catalogues. Astrometric and photometric star catalogues derived from the ESA Hipparcos Space Astrometry Mission, Publisher: Noordwijk, Netherlands: ESA Publications Division, 1997, Series: ESA SP Series vol no: 1200 (*CDS-Vizier catalog number I/239*)

Phan-Bao, N., Guibert, J., Crifo, F., Delfosse, X., Forveille, T., Borsenberger, J., Epchtein, N., Fouqué, P., & Simon, G. 2001, A&A, 380, 590

Reid, I. N., Hawley, S. L., & Gizis, J. E. 1995, AJ, 110, 1838

Reid, I. N., Liebert, J., & Schmidt, G. 2001, ApJ, 550, L61

Reid, I. N., Kilkenny, D., & Cruz, K. L. 2002, AJ, 123, 2822

Reylé, C., Robin, A. C., Scholz, R.-D., & Irwin, M. 2002, A&A, 390, 491

Salim, S., & Gould, A. 2002, ApJ, 575, L83

Scholz, R.-D., Irwin, M., Ibata, R., Jahreiss, H., & Malkov, O. Yu. 2000, A&A, 353, 958

Scholz, R.-D., Ibata, R., Irwin, M., Salvato, M., & Schweitzer, A. 2002a, MNRAS, 329, 109

Scholz, R.-D., Szokoly, G. P., Andersen, M., Ibata, R., & Irwin, M. J. 2002b, *ApJ*, 565, 539

Schweitzer, A., Scholz, R.-D., Stauffer, J., Irwin, M., & McCaughrean, M. J. 1999, *A&A*, 350, L62

Wesemael, F., Greenstein, J. L., Liebert, James, Lamontagne, R., Fontaine, G., Bergeron, P., & Glaspey, J. W. 1993, *PASP*, 105, 761

Table 1. Newly classified high proper motion stars

Star	$\mu(\text{'' yr}^{-1})$	B	R	K _s	Date of spec.	Observatory	Sp. type ¹	d(pc) ²	V _T (km s ⁻¹) ³
LSR0011+5908	1.483	...	14.5	...	2001-07-24	Lick 3m	M5.5 V	12	84
LSR0013+5437	0.981	19.4	17.4	...	2001-02-03	MDM 2.4m	DA9	26	120
LSR0014+6546	0.962	18.0	15.7	...	2001-07-24	Lick 3m	sdM4.5	40	180
LSR0020+5526	0.541	17.2	14.9	...	2001-02-03	MDM 2.4m	esdM2.5	70	175
LSR0124+6819	0.559	18.9	16.4	...	2001-12-08	Lick 3m	M7.0 V	11	29
LSR0134+6459	0.924	17.9	15.2	...	2001-12-08	Lick 3m	M5.5 V	18	78
LSR0155+3758	0.538	17.0	14.8	9.6	2001-07-24	Lick 3m	M5.0 V	20	50
LSR0157+5308	0.641	17.1	14.9	11.3	2001-02-02	MDM 2.4m	sdM3.5	45	135
LSR0200+5530	0.507	...	19.7	...	2001-02-05	MDM 2.4m	M5.5 V	90	215
LSR0212+7012	0.744	18.4	15.9	...	2001-12-08	Lick 3m	M5.0 V	40	140
LSR0258+5354	0.545	17.2	14.9	12.6	2001-02-02	MDM 2.4m	(e)sdK7	100/250	255/640
LSR0310+6634	0.808	...	17.5	...	2001-07-25	Lick 3m	DC10	60	230
LSR0316+3132	0.759	17.7	15.4	10.6	2001-12-08	Lick 3m	M5.0 V	30	105
LSR0340+5124	0.932	17.6	15.4	...	2001-02-01	MDM 2.4m	M5.5 V	18	80
LSR0342+5527	0.500	17.0	14.8	...	2001-02-04	MDM 2.4m	sdM0.0	150	350
LSR0354+3333	0.848	...	16.4	10.9	2001-02-02	MDM 2.4m	M6.0 V	20	80
LSR0358+8111	0.547	19.0	16.9	13.6	2001-12-08	Lick 3m	sdM1.5	200	515
LSR0400+5417	0.754	18.0	16.0	...	2001-02-04	MDM 2.4m	(e)sdK7	150/375	530/1330
LSR0401+5131	0.886	17.9	16.7	...	2001-02-04	MDM 2.4m	DC8	26	108
LSR0419+4233	1.535	...	17.4	...	2001-02-02	MDM 2.4m	M8.5 Ve	10	72
LSR0455+0244	0.768	18.5	16.4	...	2001-12-08	Lick 3m	M5.5 V	28	100
LSR0455+5252	0.804	...	18.3	...	2001-02-02	MDM 2.4m	M8.0 Ve	20	76
LSR0505+3043	1.097	18.5	16.0	...	2001-02-01	MDM 2.4m	esdM3.5	70	360
LSR0505+6633	0.577	...	17.0	...	2001-07-26	Lick 3m	sdM4.5	70	190
LSR0515+5911	1.015	...	16.8	...	2001-07-26	Lick 3m	M7.0 V	14	66
LSR0519+4213	1.181	...	16.1	12.9	2001-02-04	MDM 2.4m	esdM3.5	55	305
LSR0521+3425	0.512	18.1	15.8	11.0	2001-02-04	MDM 2.4m	M5.0 V	32	77
LSR0522+3814	1.703	16.6	14.5	12.6	2001-02-01	MDM 2.4m	esdM3.0	45	360
LSR0524+3358	0.530	...	17.5	14.1	2001-02-04	MDM 2.4m	(e)sdM1.5	150/250	375/625
LSR0527+3009	0.639	...	16.3	11.5	2001-02-05	MDM 2.4m	M5.0 V	40	120
LSR0533+3837	0.551	18.1	16.3	13.1	2001-02-05	MDM 2.4m	sdM2.0	150	390
LSR0539+4038	1.057	...	17.0	10.0	2001-02-01	MDM 2.4m	M8.0 Ve	10	50
LSR0541+3959	0.566	18.1	17.1	15.3	2001-02-05	MDM 2.4m	DA8	35	93
LSR0549+2329	1.379	...	17.4	...	2001-02-02	MDM 2.4m	DC8	40	260
LSR0556+1144	0.611	16.5	14.2	...	2001-12-08	Lick 3m	M5.5 V	10	29
LSR0609+2319	1.104	18.7	16.5	12.4	2001-12-08	Lick 3m	sdM5.0	45	235
LSR0618+1614	0.646	16.9	14.7	11.9	2001-02-04	MDM 2.4m	sdM2.0	85	260
LSR0621+3652	0.865	16.6	14.5	11.9	2001-02-02	MDM 2.4m	(e)sdK7	80	325
LSR0627+0616	1.019	17.6	15.4	...	2001-02-01	MDM 2.4m	esdM1.5	80	380
LSR0628+0529	0.551	...	17.1	...	2001-02-05	MDM 2.4m	M7.0 V	16	41
LSR0646+3212	0.567	...	17.5	13.1	2001-02-05	MDM 2.4m	M5.5 V	60	160
LSR0702+2154	0.653	16.9	14.9	10.3	2001-02-02	MDM 2.4m	M5.5 V	16	49
LSR0705+0506	0.510	18.8	16.0	...	2001-02-04	MDM 2.4m	sdM3.5	90	215
LSR0721+3714	0.587	18.9	16.2	10.8	2001-02-02	MDM 2.4m	M5.5 Ve	26	72
LSR0731+0729	0.512	17.3	15.2	...	2001-02-02	MDM 2.4m	M5.0 V	24	58
LSR0803+1547	0.516	18.4	16.1	13.4	2001-02-02	MDM 2.4m	(e)sdM0.0	125/275	305/670
LSR1722+1004	0.724	17.5	15.1	...	2001-07-24	Lick 3m	M4.0 V	70	240
LSR1755+1648	0.995	16.4	14.2	...	2001-07-24	Lick 3m	sdM3.5	28	130
LSR1757+0015	0.518	19.4	17.0	...	2001-07-24	Lick 3m	sdM4.5	75	180

Table 1—Continued

Star	$\mu(\text{'' yr}^{-1})$	B	R	K _s	Date of spec.	Observatory	Sp. type ¹	d(pc) ²	V _T (km s ⁻¹) ³
LSR1758+1417	1.014	16.9	15.8	14.6	2001-07-24	Lick 3m	DA10	18	86
LSR1802+0028	0.543	...	17.6	...	2001-07-26	Lick 3m	esdM1.5	180	460
LSR1806+1141	0.541	16.5	14.4	...	2001-07-26	Lick 3m	M4.0 V	45	115
LSR1808+1134	0.606	16.8	14.4	...	2001-07-26	Lick 3m	M5.0 V	18	51
LSR1809-0219	0.506	16.4	13.9	9.3	2001-07-25	Lick 3m	M4.5 V	22	52
LSR1809-0247	1.005	17.4	15.2	10.7	2001-07-25	Lick 3m	M5.0 V	26	122
LSR1817+1328	1.207	16.7	15.5	...	2001-07-25	Lick 3m	DA10	15	85
LSR1820-0031	0.555	17.8	15.7	...	2001-07-26	Lick 3m	sdM2.0	85	220
LSR1833+2219	0.502	17.6	14.9	...	2001-07-24	Lick 3m	M5.0 V	26	61
LSR1835+3259	0.747	...	16.6	9.2	2002-05-25	MDM 2.4m	M9.0 Ve	6	21
LSR1836+1040	0.921	18.2	15.9	...	2001-07-25	Lick 3m	esdM0.5	100	430
LSR1841+2421	0.752	19.0	16.5	...	2001-02-03	MDM 2.4m	M6.0 V	22	78
LSR1843+0507	0.577	19.2	17.1	...	2001-07-26	Lick 3m	M5.5 V	38	105
LSR1844+0947	0.501	17.6	15.8	...	2001-07-26	Lick 3m	(sd)M2.0 V	100/250	235/590
LSR1851+2641	0.704	18.9	16.1	...	2001-02-03	MDM 2.4m	M6.0 Ve	20	66
LSR1859+0156	0.674	16.9	14.7	...	2001-07-26	Lick 3m	M4.5 V	36	115
LSR1914+2825A	0.529	17.5	15.0	...	2001-07-26	Lick 3m	(e)sdM0.0	110/200	275/500
LSR1914+2825B	0.531	18.7	15.6	...	2001-07-26	Lick 3m	(e)sdM1.5	100/160	250/400
LSR1918+1728	0.626	...	17.2	...	2001-07-25	Lick 3m	esdM3.0	125	370
LSR1919+1438	0.507	...	14.9	...	2001-07-26	Lick 3m	M5.0 V	22	52
LSR1922+4605	0.555	17.8	15.1	12.9	2002-05-25	MDM 2.4m	(e)sdM0.0	90/200	235/520
LSR1927+6802	0.515	...	17.2	...	2002-05-25	MDM 2.4m	M6.5 V	22	53
LSR1928-0200A	0.858	...	15.2	11.3	2001-07-25	Lick 3m	M3.5 V	85	340
LSR1928-0200B	0.858	...	18.2	13.1	2001-07-25	Lick 3m	M5.5 V	65	260
LSR1933-0138	0.895	15.6	13.5	10.1	2001-07-26	Lick 3m	M3.0 V	50	210
LSR1943+0941	0.543	18.7	16.2	...	2002-05-25	MDM 2.4m	M5.5 V	26	66
LSR1945+4650A	0.612	17.9	16.8	15.5	2002-05-25	MDM 2.4m	DA9	30	86
LSR1945+4650B	0.609	19.3	17.0	15.2	2002-05-25	MDM 2.4m	DC10	60	170
LSR1946+0937	0.566	17.5	16.8	...	2001-07-26	Lick 3m	DA9	40	105
LSR1946+0942	0.555	16.8	14.6	...	2001-07-26	Lick 3m	M3.5 V	90	235
LSR1956+4428	0.891	17.3	15.0	...	2000-08-01	Lick 3m	esdM0.5	75	315
LSR2000+0404	0.503	18.0	15.7	...	2001-07-26	Lick 3m	M5.5 V	22	52
LSR2000+3057	1.339	...	15.6	9.7	2001-07-24	Lick 3m	M6.0 Ve	16	100
LSR2005+0835	0.583	16.5	14.6	...	2001-07-26	Lick 3m	(e)sdK5	100/275	275/760
LSR2009+5659	0.824	16.3	14.2	11.2	2001-07-25	Lick 3m	sdM2.0	55	215
LSR2010+3938	0.512	17.4	13.3	11.8	2000-08-01	Lick 3m	(sd)M1.5 V	100/225	240/540
LSR2013+0417	0.749	16.2	14.4	...	2001-07-25	Lick 3m	sdK7	175	615
LSR2017+0623	0.674	18.2	16.0	...	2001-07-25	Lick 3m	M5.0 V	40	125
LSR2036+5059	1.054	...	16.8	...	2001-12-09	Lick 3m	sdM7.5	18	89
LSR2044+1339	0.518	15.4	15.4	10.3	2001-07-26	Lick 3m	M5.0 Ve	16	39
LSR2050+7740	0.543	19.3	18.0	...	2002-05-20	KPNO 4m	DC11	45	115
LSR2059+5517	0.500	18.2	16.8	...	2002-05-25	MDM 2.4m	DC11	25	59
LSR2107+3600	0.736	18.4	15.9	11.7	2001-07-25	Lick 3m	M4.5 V	60	210
LSR2115+3804	0.506	17.3	15.0	12.3	2001-07-26	Lick 3m	esdK7	100	240
LSR2117+7345	0.746	18.6	16.4	...	2001-07-24	Lick 3m	M6.0 V	20	70
LSR2122+3656	0.816	18.7	16.2	...	2001-07-24	Lick 3m	esdM5.0	45	170
LSR2124+4003	0.697	17.3	14.9	...	2000-08-02	Lick 3m	M6.5 V	7	23
LSR2132+4754	0.569	16.8	14.5	10.7	2001-07-26	Lick 3m	M4.0 V	45	120
LSR2146+5147	0.584	18.5	16.0	...	2001-07-26	Lick 3m	(e)sdM1.0	105/200	290/550

Table 1—Continued

Star	$\mu(\text{'' yr}^{-1})$	B	R	K_s	Date of spec.	Observatory	Sp. type ¹	d(pc) ²	$V_T(\text{km s}^{-1})^3$
LSR2158+6117	0.819	17.9	15.7	...	2001-07-24	Lick 3m	M6.0 V	14	54
LSR2205+5353	0.528	17.3	15.1	...	2001-07-25	Lick 3m	sdM1.0	100	250
LSR2205+5807	0.538	17.9	17.6	...	2001-07-26	Lick 3m	esdM1.0	70	175
LSR2251+4706	0.631	...	17.9	12.6	2001-07-25	Lick 3m	M6.5 V	35	105
LSR2311+5032	0.669	16.9	14.6	9.9	2001-02-03	MDM 2.4m	M4.5 V	30	95
LSR2311+5103	0.531	...	18.1	12.3	2001-07-25	Lick 3m	M7.5 V	26	65
LSR2321+4704	0.712	18.5	16.2	13.2	2001-12-08	Lick 3m	esdM2.0	85	285

¹Spectral class and subtype based on spectroscopy. Parenthesis indicate change in spectral class required for consistency with the star's kinematics.

²Spectroscopic distance estimate. Stars with uncertain spectral classes have distance estimates corresponding to each of the classes, the lower estimate being that of the higher metallicity class. For the white dwarfs, this is the photometric distance estimate based on the B-R color.

³Transverse (sky-projected) velocities based on the proper motion and spectroscopic distance. Stars with uncertain spectral types are listed with velocities corresponding to both distance scales.

Table 2. Spectral Type Indexes for M dwarfs and subdwarfs

Index Name	Numerator	Denominator	Other Name	Ref.
CaH1	6380-6390	Avg. of 6410-6420 and 6345-6355	...	Reid <i>et al.</i> 1995
CaH2	6814-6846	7042-7046	...	Reid <i>et al.</i> 1995
CaH3	6960-6990	7042-7046	...	Reid <i>et al.</i> 1995
TiO5	7126-7135	7042-7046	...	Reid <i>et al.</i> 1995
VO1	7430-7470	7550-7570	VO 7434	Hawley <i>et al.</i> 2002
TiO6	7550-7570	7745-7765
VO2	7920-7960	8130-8150
TiO7	8440-8470	8400-8420	TiO 8440	Hawley <i>et al.</i> 2002
Color-M	8105-8155	6510-6560

Table 3. Blackbody temperature fits for the white dwarfs

Star	$T_{blackbody}$	Spectral type
LSR0013+5437	5500	DA9
LSR0310+6634	5000	DC10
LSR0401+5131	6500	DC8
LSR0541+3959	6000	DA8
LSR0549+2329	6000	DC8
LSR1758+1417	5250	DA10
LSR1817+1328	5000	DA10
LSR1945+4650A	5750	DA9
LSR1945+4650B	5000	DC10
LSR1946+0937	5750	DA9
LSR2050+7740	4750	DC11
LSR2059+5517	4750	DC11

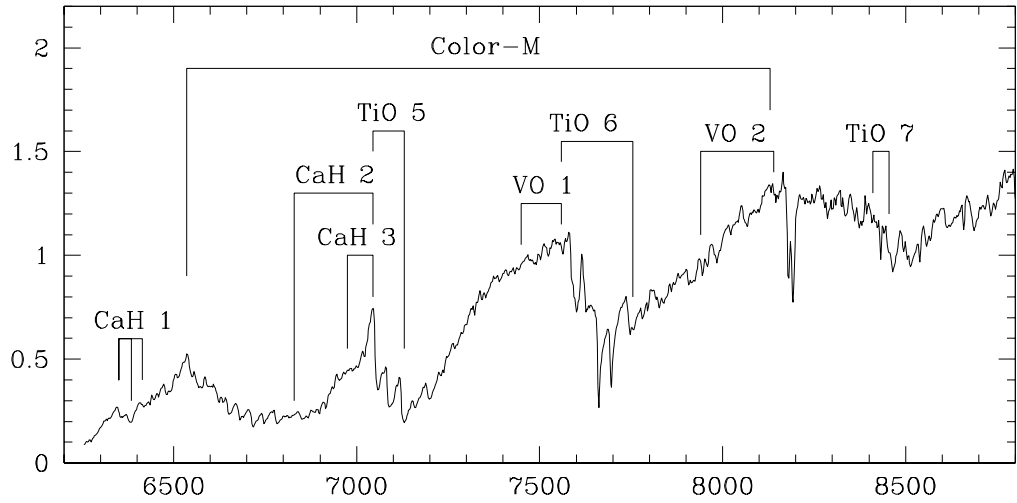


Fig. 1.— Illustration of the different spectral indexes cited in this paper, as defined in Table 1, here shown with the spectrum of the star LSR1809-0247 (M5.0 V). The indexes measure the strengths of all the most prominent molecular features in the 6000Å-9000Å range.

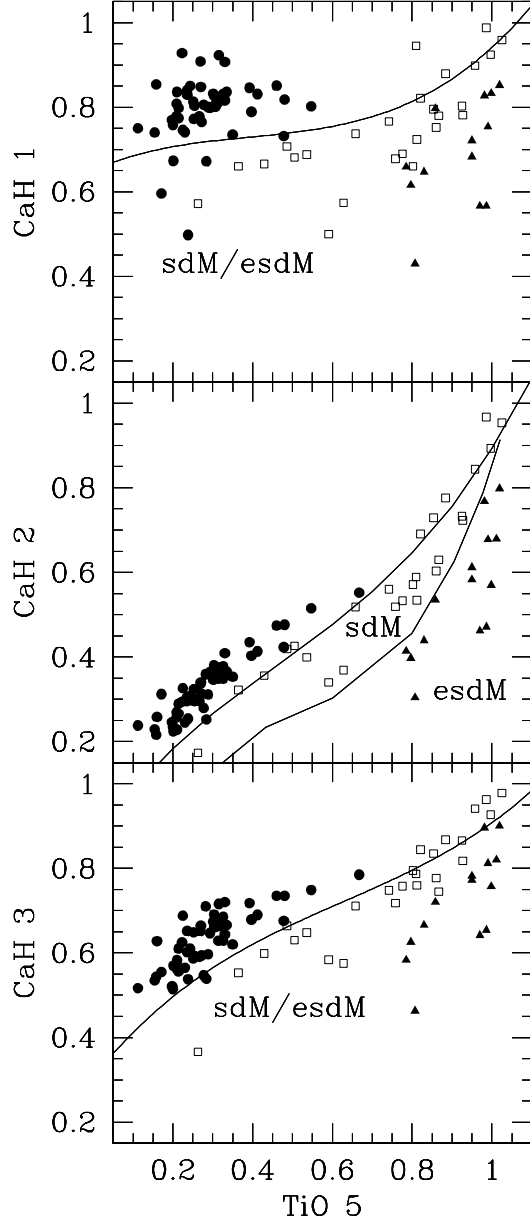


Fig. 2.— Separation of the high proper motion red dwarfs into three metallicity classes (dwarfs dM, subdwarfs sdM, extreme subdwarfs esdM) based on the ratio of the CaH spectral indexes with the TiO5 spectral index. This classification scheme is based on the criteria defined by G97. We use the CaH2/TiO5 ratio as the main criterion. The three classes show up well separated by the CaH3/TiO5 ratio. The CaH1/TiO5 ratio, on the other hand, does not discriminate as well between the dM and sdM classes; the shorter dynamic range of the CaH1 index makes classification with the CaH1/TiO5 ratio more sensitive to measurement errors.

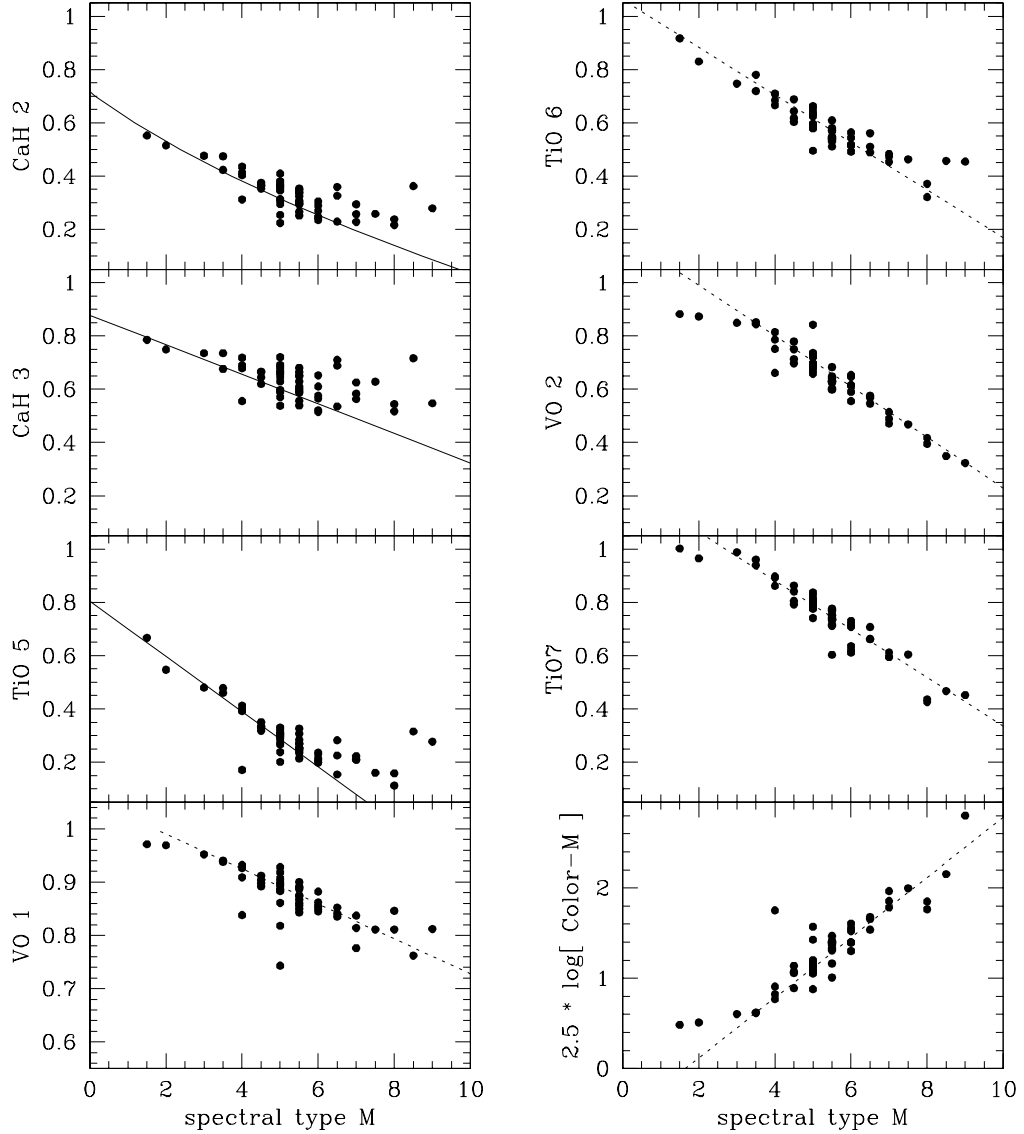


Fig. 3.— Correlation between spectral type and the different spectral indexes, for the 54 M dwarf stars classified in this paper. The relationships determined by G97 for the CaH₂, CaH₃, and TiO₅ indexes are plotted in continuous lines. New relationships for the other indexes are plotted as dotted lines. Classification of early-type M dwarfs is more reliable when the blueward indexes (CaH₂, TiO₅) are used, while late-type M dwarfs are better classified with the redward indexes (VO₂, TiO₇).

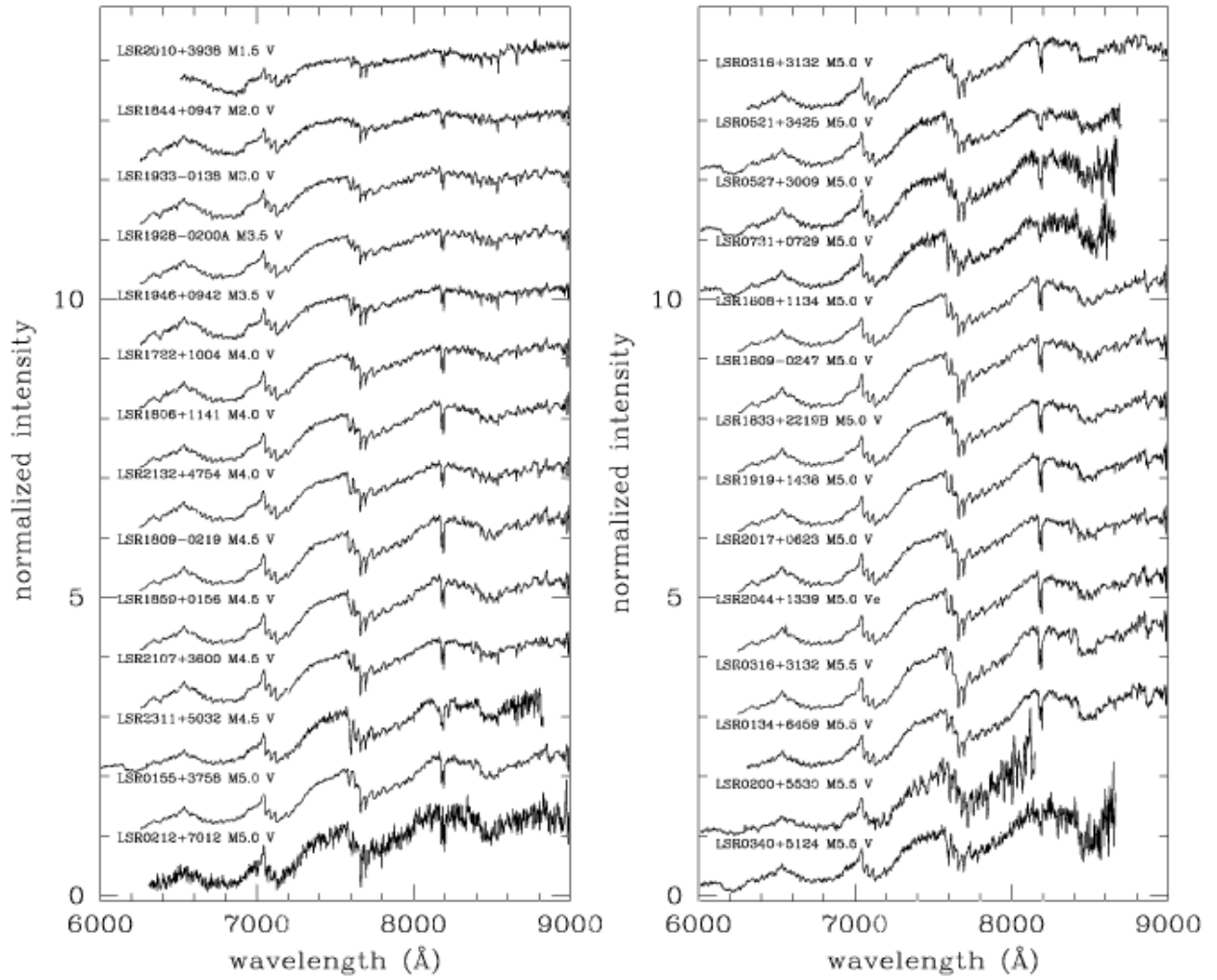


Fig. 4.— Spectral sequence for M dwarf stars classified in this paper. Spectra have been normalized to 1.0 at 7500Å and shifted vertically by integer values for clarity. The later-type stars are displayed on Figure 5.

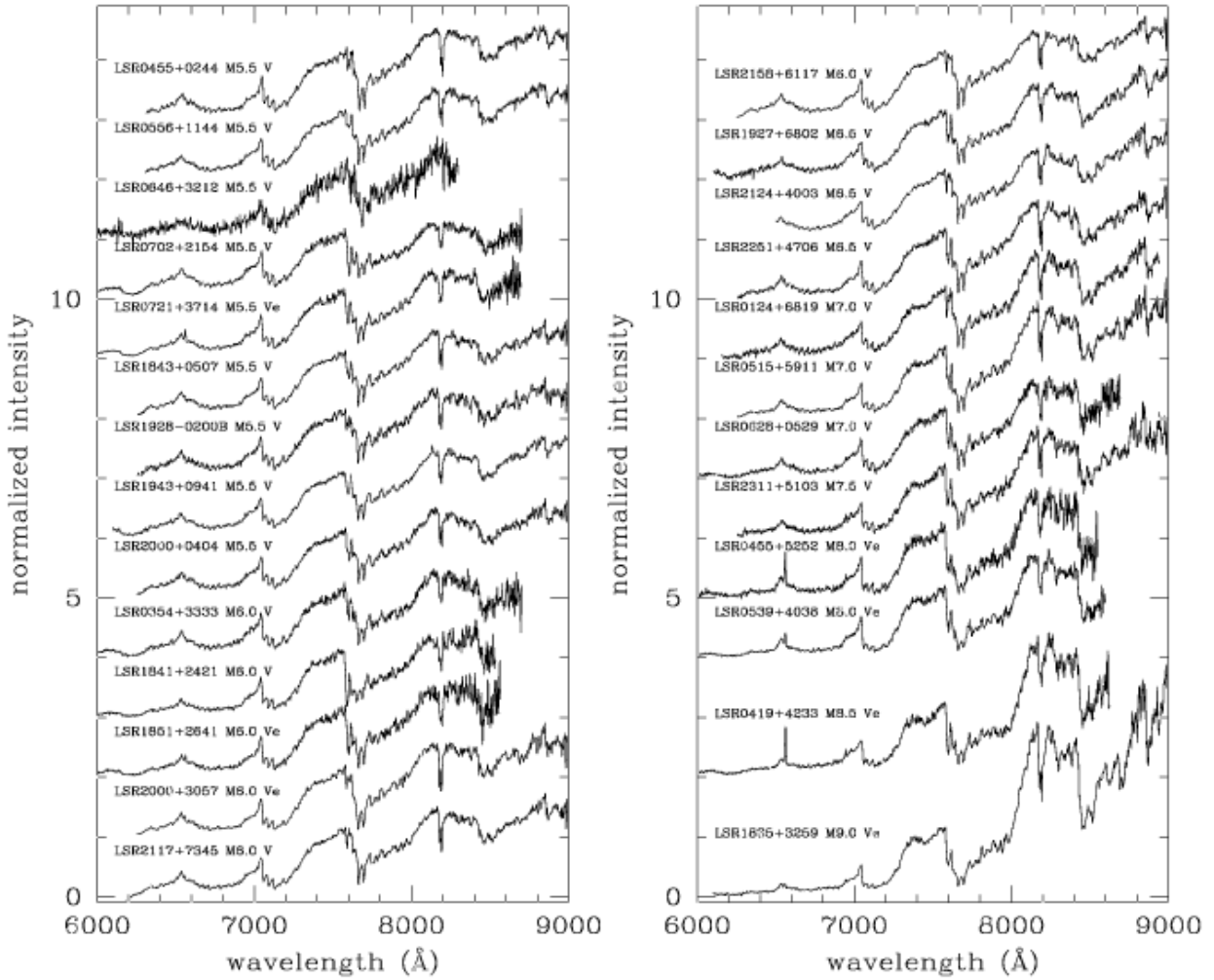


Fig. 5.— Spectral sequence for M dwarf stars classified in this paper, continued from Figure 4.

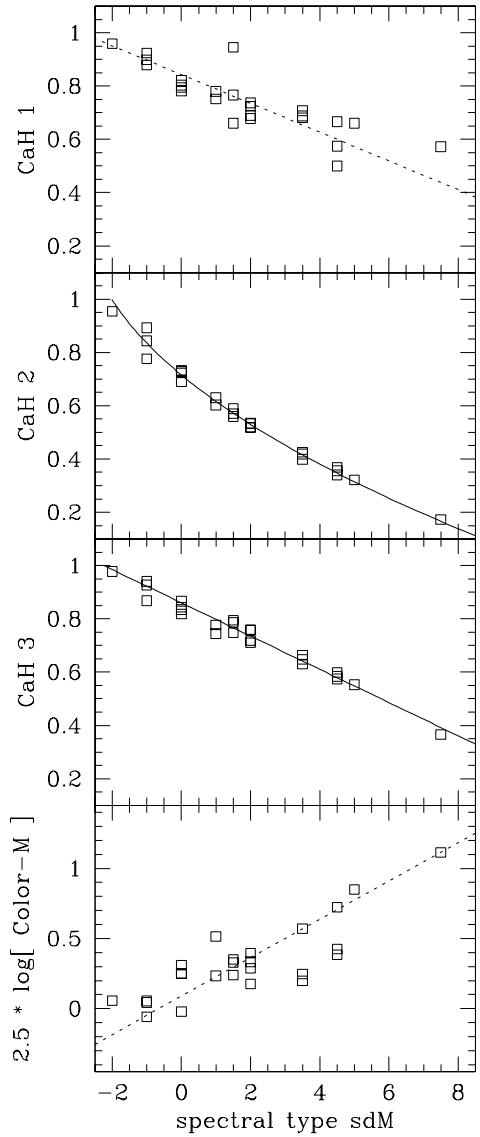


Fig. 6.— Classification of the subdwarfs based on spectral features. Classification is based of the CaH2 and CaH3 spectral indexes. The relationships determined by G97 are plotted in dotted lines. Values of the CaH1 index and of the Color-M index are plotted against spectral type for comparison.

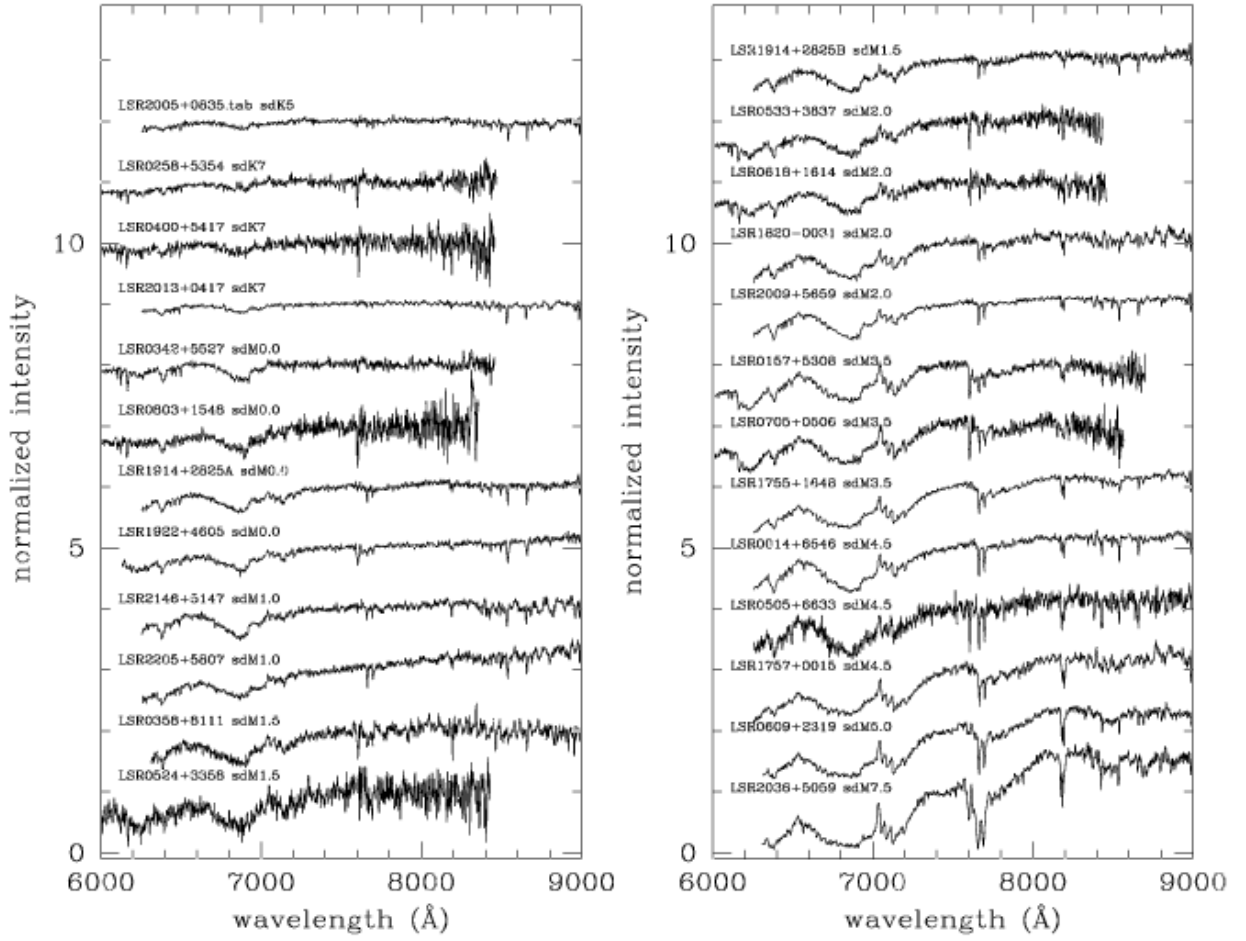


Fig. 7.— Spectral sequence for subdwarf (sdM) stars classified in this paper. Spectra have been normalized to 1.0 at 7500Å and shifted vertically by integer values for clarity.

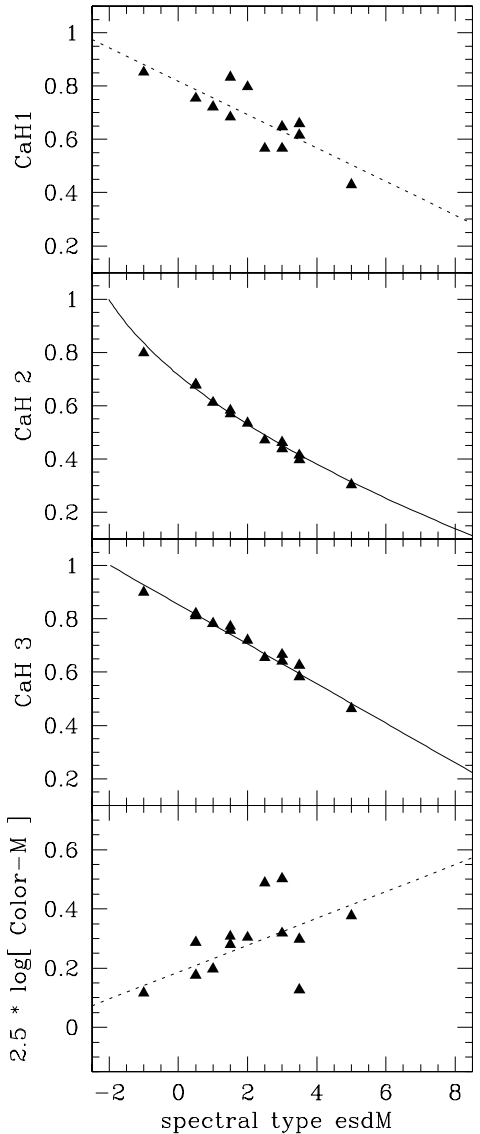


Fig. 8.— Classification of the extreme subdwarfs based on spectral features. Classification is based of the CaH2 and CaH3 spectral indexes. The relationships determined by G97 are plotted in dotted lines. Values of the CaH1 index and of the slope of the continuum index are plotted against spectral type for comparison.

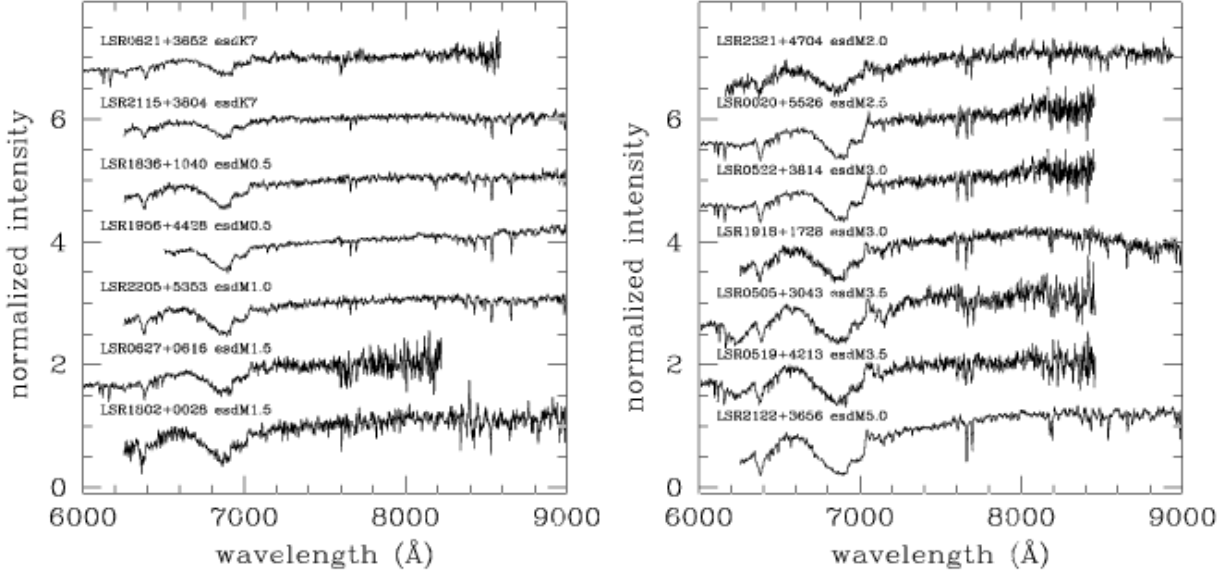


Fig. 9.— Spectral sequence for extreme subdwarf (esdM) stars classified in this paper. Spectra have been normalized to 1.0 at 7500Å and shifted vertically by integer values for clarity. Several spectra are very noisy because we used a spectroscopic setup optimized for the observation of red dwarfs.

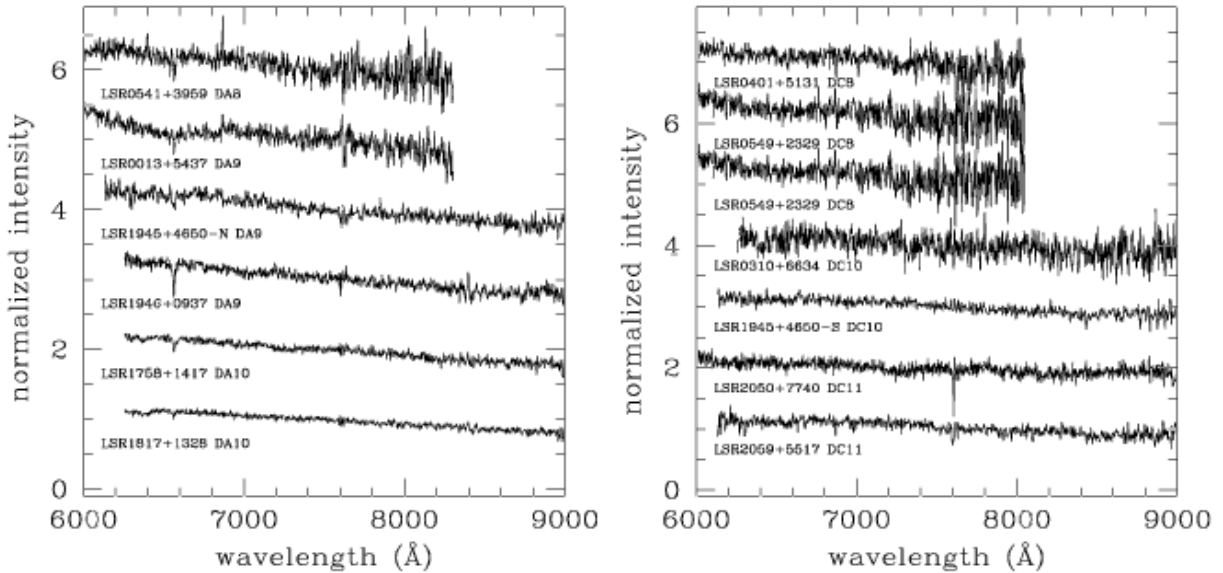


Fig. 10.— Spectra of the white dwarfs found in the sample of new high proper motion stars. All the spectra are normalized to 1.0 at 7500Å, and shifted by integer values on the vertical scale for clarity.

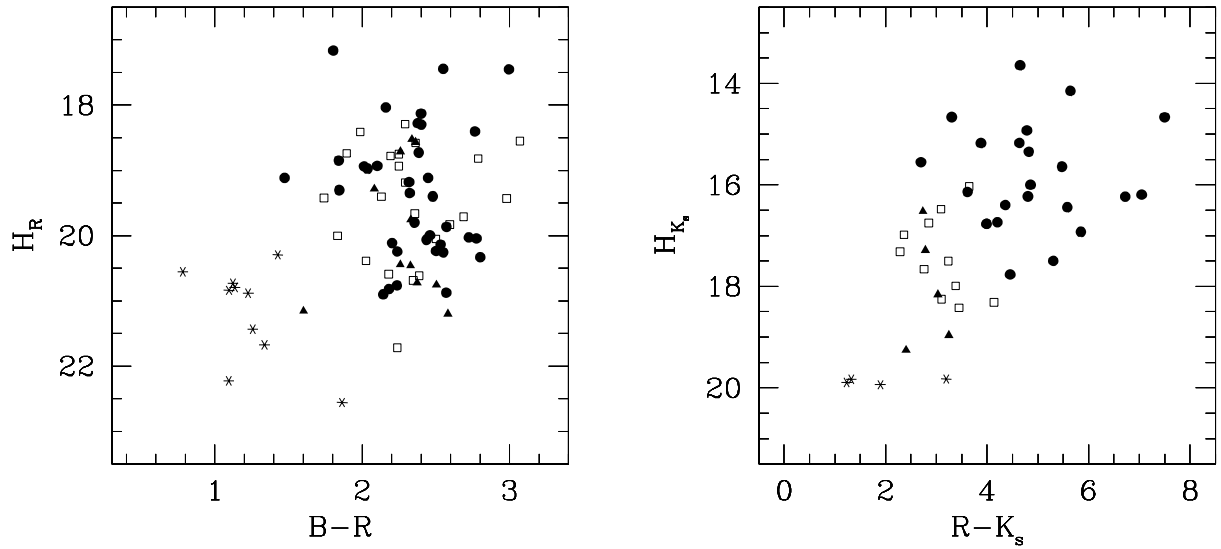


Fig. 11.— Reduced proper motion diagrams for the stars classified in this paper. The reduced proper motion terms are derived from $H_R = R + \log \mu + 5$, and $H_{K_s} = K_s + \log \mu$, where μ is the proper motion of the star. Red dwarfs are represented by filled circles, subdwarfs (sdM) by open squares, extreme subdwarfs (esdM) by filled triangles, and white dwarf by asterisks.

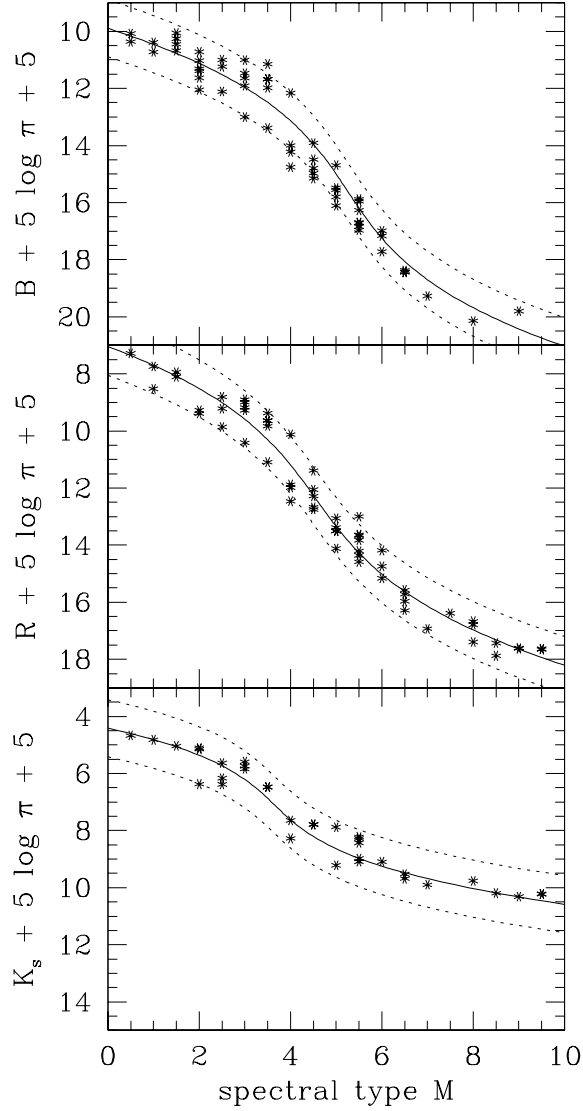


Fig. 12.— Empirical spectral-type / absolute magnitude relationship for a sample of nearby M dwarfs with assigned spectral types and measured geometric parallaxes (π). The observed B and R magnitudes are those recorded on the IIIaJ (blue) and IIIaF (red) POSS-II plates as listed in the Second Guide Star Catalog (GSC2.2.1), the K_s magnitudes are from the 2MASS Second incremental Release. The relationships (continuous lines) are determined from third order polynomial fits. Most stars fall within 1 magnitude of the adopted relationship (dashed lines).

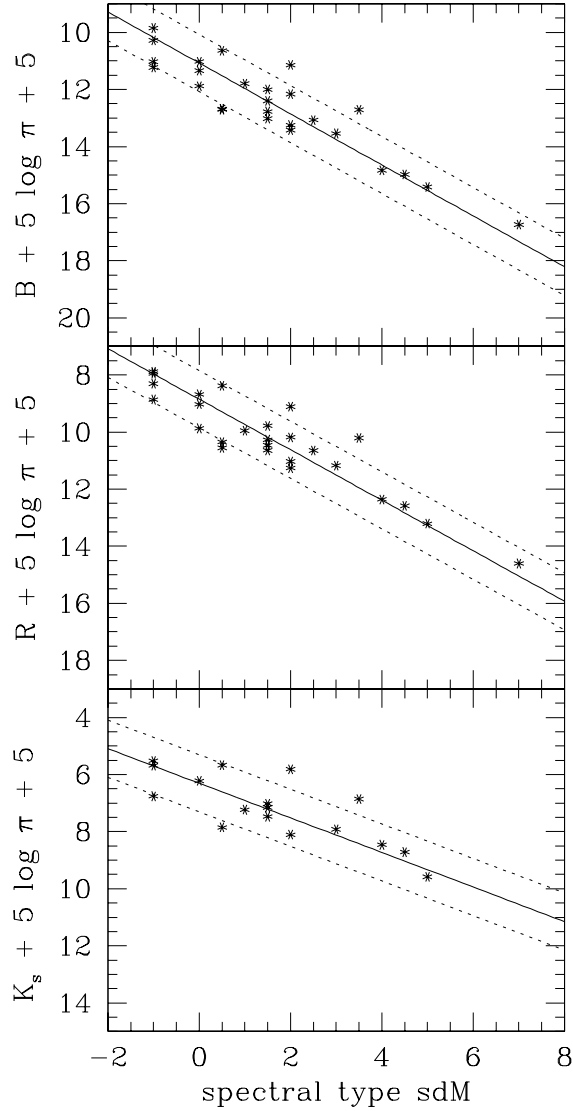


Fig. 13.— Empirical spectral-type / absolute magnitude relationship for a sample of sdM dwarfs with assigned spectral types and measured geometric parallaxes (π). The observed B and R magnitudes are those recorded on the IIIaJ (blue) and IIIaF (red) POSS-II plates as listed in the Second Guide Star Catalog (GSC2.2.1), the K_s magnitudes are from the 2MASS Second incremental Release. The linear relationships (continuous lines) are determined from first order polynomial fits. Dashed lines mark the 1 magnitude scatter.

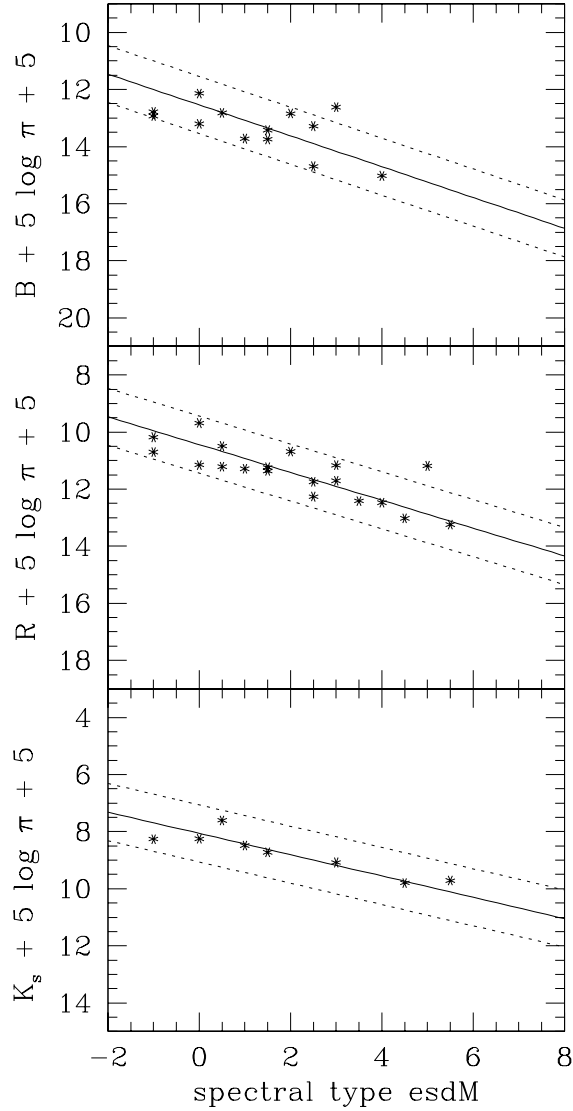


Fig. 14.— Empirical spectral-type / absolute magnitude relationship for a sample of esdM dwarfs with assigned spectral types and measured geometric parallaxes (π). The observed B and R magnitudes are those recorded on the IIIaJ (blue) and IIIaF (red) POSS-II plates as listed in the Second Guide Star Catalog (GSC2.2.1), the K_s magnitudes are from the 2MASS Second incremental Release. The linear relationships are determined from first order polynomial fits. Dashed lines mark the 1 magnitude scatter.

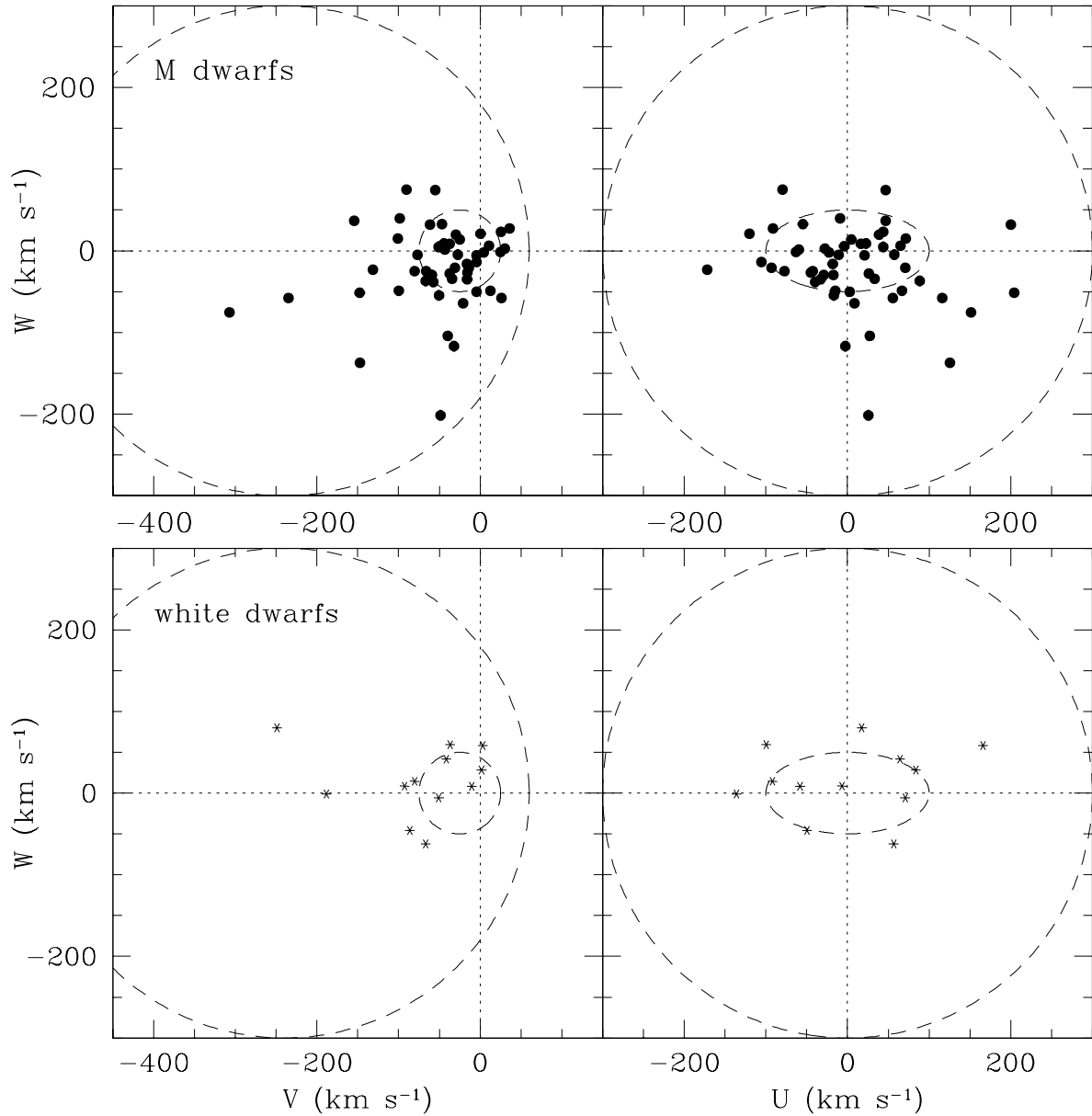


Fig. 15.— UVW velocity space distribution of the new M dwarfs (top) and white dwarfs (bottom), assuming a radial velocity of zero. The dashed lines show the typical range of the disk and halo stars.

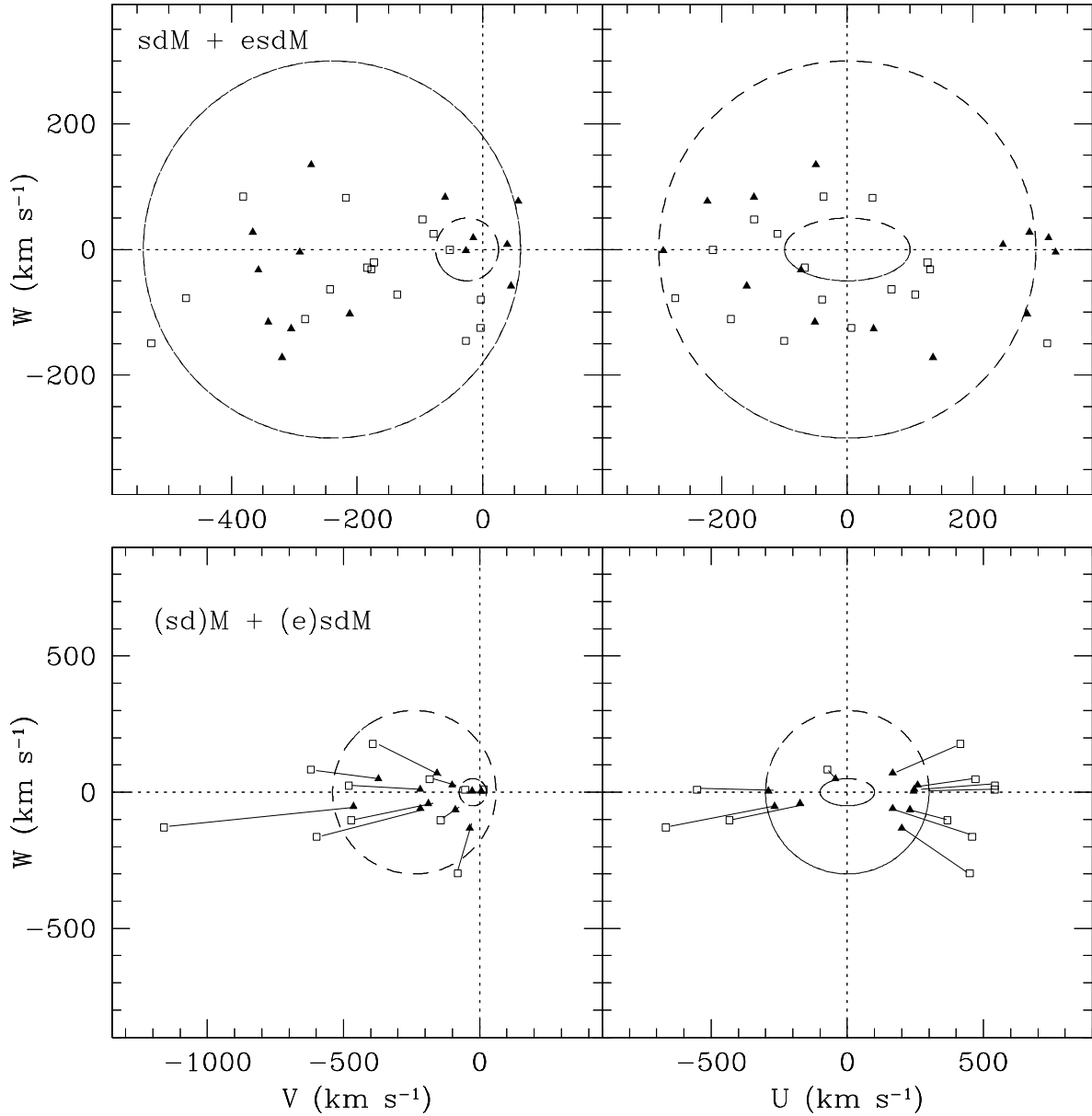


Fig. 16.— Top: UVW velocity space distribution of the new subdwarfs (open squares) and extreme subdwarfs (filled triangles). A radial velocity of zero is assumed. Bottom: UVW velocity space distribution of stars whose spectra is consistent with a distant dM or sdM star, but whose kinematics is more consistent with an sdM or esdM star at a closer distance. Each star is shown with both the larger (open squares) and smaller (filled triangle) distance scale.